ELSEVIER

Contents lists available at ScienceDirect

Science of the Total Environment

journal homepage: www.elsevier.com/locate/scitotenv





Imprint of incomplete combustion processes on the water column of the anthropogenic-pressured Baltic Sea

Tassiana S.G. Serafim^{a,*}, Detlef E. Schulz-Bull^a, Christopher P. Rüger^{b,c}, Thorsten Dittmar^{d,e}, Jutta Niggemann^d, Ralf Zimmermann^{b,c}, Joanna J. Waniek^a, Helena Osterholz^a

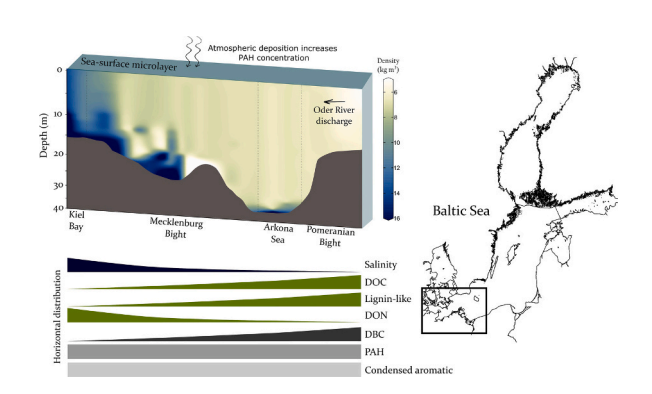
- ^a Leibniz Institute for Baltic Sea Research Warnemiinde (IOW), Rostock, Germany
- ^b Department Life, Light & Matter, University of Rostock (LLM), Rostock, Germany
- ^c Joint Mass Spectrometry Centre (JMSC), Chair of Analytical Chemistry, University of Rostock, Rostock, Germany
- d Research Group for Marine Geochemistry, Institute for Chemistry and Biology of the Marine Environment (ICBM), Carl von Ossietzky Universität Oldenburg, Oldenburg, Germany
- e Helmholtz Institute for Functional Marine Biodiversity (HIFMB) at the Carl von Ossietzky Universität Oldenburg, Oldenburg, Germany

HIGHLIGHTS

Different analytical methods revealed varying thermogenic organic matter distribution patterns in the Baltic Sea.

- Ultra-high-resolution mass spectrometry indicated a mixture of land-based sources and anthropogenic pressure from ship emission.
- Dissolved black carbon concentrations are higher in the Baltic Sea than in other coastal systems.

GRAPHICAL ABSTRACT



ARTICLE INFO

Editor: Kevin V Thomas

Keywords:
Polycyclic aromatic hydrocarbon
Dissolved black carbon
Dissolved organic matter
Baltic Sea
FT-ICR-MS
Pyrogenic organic matter

ABSTRACT

This study evaluates the distribution and sources of thermogenic organic matter in the Baltic Sea water column, focusing on polycyclic aromatic hydrocarbons (PAH), dissolved black carbon (DBC), and the imprint of thermogenic organic matter on the dissolved organic matter (DOM) pool. The spatial patterns and complex interactions between land-based and atmospheric sources were assessed from Kiel Bay to Pomeranian Bight within the water column with the combined targeted and untargeted approaches. The findings emphasize the significant influence of terrestrial inputs from the Oder River and autochthonous production composing DOM. In the Pomeranian Bight, PAH and DBC concentrations strongly correlate with land-based discharge, while shipping emissions play a more prominent role in the Arkona Sea. The sea surface microlayer shows unique characteristics in DOM composition, with potential combustion products as an important source revealed by PAH and DOM analyses. Ultrahigh-resolution mass spectrometry identified combustion products, in the DOM pool, providing insights into anthropogenic impacts. This research contributes to a better understanding of the complex

E-mail address: tassiana.sgs@gmail.com (T.S.G. Serafim).

https://doi.org/10.1016/j.scitotenv.2025.178537

^{*} Corresponding author.

dynamics of thermogenic organic matter in coastal environments, highlighting the interplay between land-based sources, shipping emissions, and in-situ processes in the Baltic Sea region.

1. Introduction

The presence of thermogenic organic matter in coastal environments, influenced by riverine transport and atmospheric deposition, can be attributed to both shipping activities (Kanwischer et al., 2020; Hermansson et al., 2021), and land-based sources that can reflect historical biomass burning in the drainage basins (Dittmar et al., 2012; Marques et al., 2017; Fang et al., 2021; Serafim et al., 2023) and the use of biomass for energy production (Wang et al., 2020; Ljung et al., 2022). The combination of these diverse sources can result in a complex mixture of thermogenic organic compounds in coastal environments, highlighting the multifaceted nature of anthropogenic impact on marine ecosystems. Hence, these products of incomplete combustion play a significant role in the global carbon cycle and climate change (Li et al., 2016; Coppola et al., 2018; Ljung et al., 2022), with ubiquitous distribution in the environment due to extensive anthropogenic pressure (Bond et al., 2013; Kanwischer et al., 2020).

Combustion products are regularly assessed via pyrogenic/petrogenic/thermogenic tracers such as polycyclic aromatic hydrocarbons (PAH) and black carbon (BC), often analyzed through its molecular markers (benzene polycarboxylic acids, BPCA). These tracers of anthropogenic impact are applied across various environmental matrices, e.g., soil, aerosols, freshwater systems, seawater, and sediments (Yunker et al., 2002; Glaser and Amelung, 2003; Dittmar et al., 2012; Saiz et al., 2015; Santín et al., 2016; Marques et al., 2017; Kanwischer et al., 2020; Serafim et al., 2023; Zhang et al., 2024). Although PAH and BC are both used to quantify polycyclic aromatic compounds, it is important to note that they cover different analytical windows, with BC providing more information quantifying polycyclic structures more complex and larger than PAH, offering a better understanding of thermogenic organic matter concentrations and environmental distribution (Wiedemeier et al., 2015). With PAH being considered as molecular precursors of BC (Lima et al., 2005) and also presenting similar sources, their interaction in the environment can vary. Ljung et al. (2022) combined PAH and BC measurements to assess the historical trends of anthropogenic pressure in sediments in the Baltic Sea area. The authors did not find a correlation between the two thermogenic organic matter tracers, which could indicate different mechanisms and sources controlling their deposition in the sedimentary compartment. Different trends were observed elsewhere, where the distribution of PAH was driven by BC concentrations in the sediment (Sánchez-García et al., 2010; Li et al., 2016). Therefore, the two approaches can be coupled to provide insights on sources and transport or preservation mechanisms within specific environmental settings.

The apportionment of thermogenic organic matter was recently addressed by using an untargeted approach: ultrahigh-resolution mass spectrometric analysis, with assessment of thermogenic signatures in the extractable phase in sediments (Downham et al., 2024), in aerosols (H. Bao et al., 2023; M. Bao et al., 2023; Schneider et al., 2023), and in dissolved organic matter (DOM; Dittmar and Koch, 2006; Zhao et al., 2023; H. Bao et al., 2023; M. Bao et al., 2023). In DOM, the anthropogenic imprint was first identified by Dittmar and Koch (2006), where over 200 different PAH were present in marine DOM, indicating a substantial presence of thermogenic compounds in deep-sea environments. Furthermore, Zhao et al. (2023), H. Bao et al. (2023) and M. Bao et al. (2023) assessed the imprint of DBC in marine DOM, by using the chemical characteristics derived from DOM characterization. The combination of the targeted and untargeted approaches may provide information on the sources and processes of thermogenic organic matter at molecular level in the DOM pool.

The presence and distribution of thermogenic organic matter in the

water column can vary due to various processes that can remove thermogenic substances from the dissolved fraction of the water column. These processes include photodegradation, biodegradation, and adsorption onto sinking particles (Stubbins et al., 2012; Nakane et al., 2017; Wagner et al., 2018). It is known that photodegradation is the primary removal mechanism, while biodegradation can be more prominent in water columns with high turbidity (Seidel et al., 2015). In areas with high ship traffic density or frequent wildfires where the atmospheric deposition plays a crucial role, the accumulation of thermogenic organic matter in the sea surface microlayer (SML) can be enhanced. The SML is a thin (up to 1 mm), highly dynamic, complex, and heterogeneous layer that is influenced by environmental conditions (e.g., wind, precipitation) and chemical properties (e.g., presence of surfactants). It plays an essential role in the global distribution of anthropogenic pollutants (Cunliffe and Wurl, 2014). Data on DBC in the SML in coastal areas is scarce (Mari et al., 2017; Pradeep Ram et al., 2018; Vaezzadeh et al., 2023), while PAH concentrations have been documented in various marine ecosystems with high anthropogenic pressure (Witt, 2002; Guitart et al., 2007; Manodori et al., 2006; Lim et al., 2007; Wurl and Obbard, 2004; Ya et al., 2014; Huang et al., 2020), where the partitioning between dissolved and particulate phases varied.

The Baltic Sea, due to the high anthropogenic pressure, has been studied over the last decades for several organic pollutants, with thermogenic organic matter being investigated via PAH (Witt, 2002; Kanwischer et al., 2020; Naumann et al., 2020; Naumann et al., 2023), and being a result of land-based sources from river discharge in addition to shipping emission. Witt (2002) analyzed PAH in different areas of the Baltic Sea and within the surface water. The author found a seasonal variation in the PAH concentrations, with SML enriched in PAH. Later, Kanwischer et al. (2020), while evaluating winter historical data (2003–2018), could see a trend in increasing concentrations of PAHs in Kiel Bay and Pomeranian Bight. No DBC data for the Baltic Sea is available. Therefore, this study aims to assess the sources of pollutants in the dissolved fraction of water by using targeted and untargeted methods to analyze the thermogenic organic matter and its imprint in the DOM, from the southwestern Baltic Sea to the Pomeranian Bight. This approach will provide valuable information about how thermogenic organic matter is transported in coastal seas, as well as their distribution and sources in the water column. By combining the analysis of specific tracers with DOM characterization, we aim to contribute to a better understanding of the distribution and behavior of organic matter in coastal environments, specifically those of thermogenic origin.

2. Material and methods

2.1. Study area and sampling strategy

The Baltic Sea is a semi-enclosed brackish water body that is considered one of the most polluted seas worldwide (Narloch et al., 2022; Ytreberg et al., 2022). Due to the permanent anthropogenic pressure, the Baltic Sea ecosystem suffers from acidification, eutrophication, and anoxic waters (Gustafsson et al., 2012; Meier et al., 2019). Connected to the North Sea via the narrow Danish Straits the Baltic Sea receives only sporadic inflows from the North Sea, resulting in a long water residence time of around 30 years (Seidel et al., 2017; HELCOM, 2018), which indirectly facilitates the accumulation of material discharged by the rivers (Deutsch et al., 2012; Naumann et al., 2020). The average water depth of the shallow system is 52 m, with the upper 40 m of the water column well mixed by physical processes such as convection and turbulence by wind during winter (Kanwischer et al., 2022; Feistel et al., 2008). Strong stratification and lack of inflow can lead to

stagnation in the deeper basins, where water exchange is restricted by sills.

Water samples were taken in spring 2023 (from 31 March to 12 April) on expedition EMB315 of RV Elisabeth Mann Borgese in the southwestern Baltic Sea to Pomeranian Bight ($10^{\circ}0' E - 54^{\circ}3' N$ and $14^{\circ}5'$ $E - 54^{\circ}0'$ N; Fig. 1). The samples were taken near the shipping lanes, with distances between 0 and 36 km to a shipping traffic density of at least 15,000 vessels crossing a 1×1 km grid cell per year (HELCOM, 2021). The water column was profiled at each station via CTD, and subsurface water (SSW) at 1 m and deep layers were sampled. If feasible, sea surface microlayer (SML) samples and the corresponding reference SSW were obtained from the working boat maneuvered upwind of the research vessel. The SML samples were taken using the glass plate technique described in Harvey and Burzell (1972) and tested later by Zhang et al. (2003). It is important to highlight the effectiveness of the glass plate technique in the analysis of PAH in the SML (Guitart et al., 2004). During the sampling campaign, the thickness of the sampled layer was, on average, $64.7 \pm 2.6 \, \mu m$, where thickness is a result of the sample volume in cm³ multiplied by 10⁴, divided by the immersed area of the plate in cm² multiplied by the number of dips per sample (Cunliffe and Wurl, 2014). The SML thickness average during sampling corresponds to reported values (Zhang et al., 2003), where the authors determined an SML thickness for natural seawater of 50 \pm 10 μ m. High-salinity water inflowing from the North Sea observed at some western stations was not sampled. Physical-chemical parameters such as salinity, temperature, and depth were obtained through the sensors of the CTD rosette (Seabird SBE 911 plus). Wind direction and speed, and humidity were obtained from the research vessel's weather station as hourly averaged data. Sampling sites were grouped into four distinct areas: Kiel Bay, Mecklenburg Bight, Arkona Sea, and Pomeranian Bight, according to Witt (2002), Kuss et al. (2020), Neumann et al. (2020), Naumann et al. (2023), and the wind direction.

All glassware used in all the procedures was thoroughly cleaned with acidified water, rinsed several times with ultrapure water, and prebaked at 400 °C for 4 h to remove any organic residues. GF/F filters (Whatman, pore size $0.7 \mu m$) were pre-combusted at $400 \,^{\circ}$ C and used to separate the suspended particulate material to the dissolved fraction. The water samples were filtered and aliquots were separated for nutrient analysis, dissolved organic carbon (DOC) and total dissolved nitrogen (TDN), DOM characterization, DBC and PAH. Nutrient concentrations (nitrate, nitrite, phosphate, and silicate) were obtained by applying a simultaneous photometric method via automated Continuous Flow Analyzer (CFA; Alliance Instruments, Austria); precision and detection limits were 0.21 μ mol L⁻¹, 0.022 μ mol L⁻¹, 0.034 μ mol L⁻¹, and 0.71 μmol L⁻¹ for nitrate, nitrite, phosphate, and silicate, respectively. All analyses were done following accredited protocols (D-PL-14544-01-00). DOC concentrations, TDN concentrations, and recoveries for the solid phase extraction (see section 'DOM characterization') were acquired via total organic carbon analyzer (TOC-L, Shimadzu). Dissolved organic nitrogen (DON) was calculated using TN minus nitrate and nitrite species concentrations.

2.2. PAH quantification

The sixteen PAH designated as high-priority pollutants by the Environmental Protection Agency (EPA) were isolated using solid-phase extraction (SPE), as described by Li et al. (2015), with modifications. One liter of filtered seawater was acidified to pH 2 with HCl (Suprapur 30 %, Merck), and 0.1 % methanol was added to the sample to improve the extraction. Next, the sample was passed through ENVI-18 cartridges (500 mg, Merck) previously conditioned with 10 mL of dichloromethane, 10 mL of methanol, and 10 mL of ultrapure water at a flow rate of 4 mL min⁻¹. The cartridges were immediately desalinated with acidified (pH 2) ultrapure water, and stored at -20 °C for further

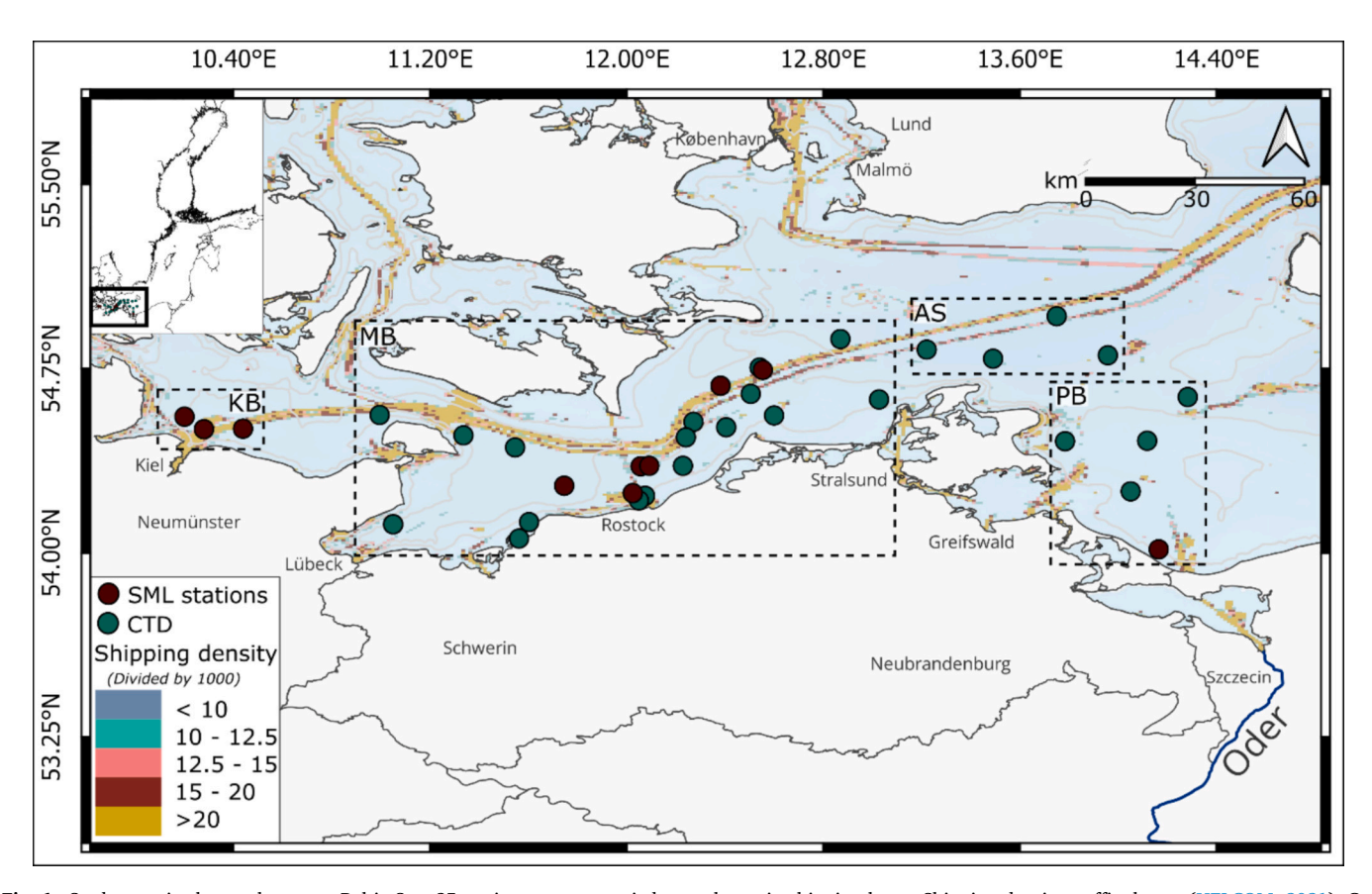


Fig. 1. Study area in the southwestern Baltic Sea: 25 stations were occupied near the main shipping lanes. Shipping density traffic, layers (HELCOM, 2021). Coordinate system: ETRS89 (EPSG:4258).

analysis. The cartridges were dried with $N_{2,}$ the analytes eluted with 12 mL of DCM and concentrated in an evaporation system at 40 °C under clean air purge (5.0 bar), where hexane (2 mL) was added twice for solvent exchange. The samples were then concentrated to 150 μ L by a rotary evaporator system (200 mbar, at 30 °C and 90 rpm) and spiked with the deuterated PAH as an internal standard and quantified using a GC–MS (Agilent 5977).

The sample preparation method was thoroughly validated through a recovery investigation process. Seawater, spiked seawater and spiked ultrapure water samples were filtered and extracted via the SPE method, and recovery values were obtained. Quality control measures were taken by processing procedural blanks, matrix spikes, and sample duplicates. An external standard method utilizing a 16 PAH reference material mixture was applied. The calibration curve had 12 levels with concentrations ranging from 0.5 to 250 pg μL^{-1} and a coefficient of determination (R²) between 0.992 and 0.999. The recoveries and relative standard deviation (RSD) ranged from 87.35 to 99.9 % (n = 13; average: 95.0 \pm 3.5 %) and 3.2 to 34.2 %, respectively. The concentrations were corrected by the recovery values from the recovery test. The limit of detection varied between 0.01 and 0.03 ng L^{-1} . The analytical errors for PAH concentration were, on average, 2 %. The procedure blanks were, on average, 2.34 ng L^{-1} . The sources for PAH in environmental samples are commonly assessed by developed diagnostic ratios between the concentrations of single PAH with similar physicochemical properties (Yunker et al., 2002), with some limitations due to environmental processes (Jacobs et al., 2008).

2.3. DOM characterization

SPE was also used to isolate DOM for molecular characterization and DBC quantification (described in section 'DBC determination') with cartridges containing a styrene-divinylbenzene polymer modified with a proprietary nonpolar surface (Bond Elut PPL, 200 mg, Agilent; Dittmar et al., 2008). Before use, the cartridges were cleaned and before extraction conditioned with two cartridge fillings of methanol and two cartridge fillings of acidified water (pH 2). The filtered samples were acidified to pH 2, and after extraction, the cartridges were desalted with pH 2 ultrapure water (6 mL) and frozen. Then, the cartridges were dried with N₂ gas and eluted with 4 mL of methanol. To validate the extraction efficiency, aliquots of the methanol extracts were dried and redissolved with acidified water, and the DOC concentration of the extract was determined as described for environmental samples. On average, the PPL cartridges recovered 63 \pm 3 % (n=84) of DOC.

FT-ICR-MS analysis of the DOM extracts was performed on a SolariX instrument equipped with a 7 T superconducting magnet (Bruker Daltonik, Bremen, Germany). The extracts were diluted with ultrapure water and methanol (1:1, v/v) to a concentration of 417 µM of organic carbon (OC). The samples were injected into the ESI source in negative ionization mode (ESI-), with a voltage of 3.4 kV, and for each measurement, 250 scans were co-added covering a mass range from 100 to 1000 Da with a 2 s (4 megaword) transient, at a flow rate of 200 μ L h⁻¹. The spectra were mass-calibrated with an internal list in the Bruker Daltonics Data Analysis software (version 5.0 SR1). Masslists were exported at S/N=0 and submitted to formula assignment using ICBM Ocean (Merder et al., 2020) within the elemental limits of ¹²C (1–50), ¹H (1-100), $^{16}{\rm O}$ (1-50), $^{14}{\rm N}$ (1-4), and $^{32}{\rm S}$ (1-2) and isotopic verification, and peaks with an error threshold of ± 0.5 ppm were considered for analysis. The intensity-weighted average molecular weights, double bond equivalents (DBE), H:C ratios, O:C ratios, compound group definitions, and aromaticity index were calculated for each sample. The modified aromaticity index (AI_{MOD}) and double-bound equivalence (DBE) are proxies for aromatic character of the molecular formulae (MF) (Koch and Dittmar, 2006; Riedel et al., 2012). The molecular compounds group for condensed aromatic compounds assignment was done by considering an $\mathrm{AI}_{\mathrm{MOD}}$ higher than 0.66 from DOM chemical characteristics (Dittmar and Koch, 2006), while the terrestrial index (I_{TERR})

was calculated from Medeiros et al. (2016), where 184 MF were suggested as indicators of riverine inputs.

2.4. DBC determination

DBC was determined at the molecular level via BPCAs produced after OM oxidation (Dittmar, 2008; Stubbins et al., 2015). The method for dissolved black carbon analysis has been continually updated and the applicability of DBC as a tracer for pyrogenic or thermogenic organic matter has repeatedly been challenged. As strongly recommended previously (Kappenberg et al., 2016; Bostick et al., 2018; Wagner et al., 2018; Barton et al., 2024), the less carboxylated BPCAs (3 and 4 carboxylic groups) should not be used for the BC assessment due to their potential production from non-pyrogenic material, leading to an overestimation of the BC content. Pentacarboxylic and melitic acid, B5CA and B6CA, respectively, however, are not produced from non-pyrogenic processes even when digesting samples with >5 mg of carbon (Kappenberg et al., 2016). Therefore, they are currently the two robust groups used to estimate DBC (Stubbins et al., 2015; Marques et al., 2017; Bostick et al., 2018; Wagner et al., 2018; Coppola et al., 2019; Yamashita et al., 2021). The BPCAs are defined by the single benzene ring bonded with carboxyl groups (Zhao et al., 2023). Briefly, 5 umol DOC of the extracts were added into glass ampoules, dried over night at 50 °C, and redissolved in 0.5 mL of nitric acid (Fluka, 65 %). The oxidation process happens under high pressure; therefore, the glass ampoules were sealed and placed in a stainless-steel pressure bomb in the oven at 170 °C for 9 h. After the oxidation, $450~\mu L$ of the extract was transferred into HPLC vials, where the acid was evaporated under N2 flow at 60 °C. The samples were then redissolved with 100 µL of phosphate buffer (addition of Na₂HPO₄ and NaH₂PO₄ in ultrapure water) stored at -20 °C and quantified on a Waters Acquity UPLC (Ultra Performance Liquid Chromatography) system composed of a binary solvent manager, a sample manager, a column manager, and a photodiode array light absorbance detector (PDA eA). DBC concentration was calculated according to Stubbins et al. (2015), using the concentrations of B5CA and B6CA. The ratio between the two BPCA (B6CA:B5CA) was used as a proxy for the degree of condensation (Dittmar, 2008). The calibration curve had 9 levels with concentrations ranging from 0.4 to 100 µM, and an R² between 0.9996 and 1.000. For quality control of the measurements, the reference sample Suwannee River natural aquatic organic matter (#2R101N) from the International Humic Substance Society was used. Based on the replicates of the reference sample, the analytical error for BPCA concentration was, on average, 7.5 and 7.7 % for B5CA and B6CA, respectively.

2.5. Data analysis

Indicator species analysis (ISA) was used to identify characteristic MF from the DOM characterization via FT-ICR-MS along the southwestern Baltic Sea horizontally and vertically. For all assigned MF values within the mass spectra, we calculated indicator values by multiplying the relative abundance with the relative frequency of a MF within a predefined group: for horizontal distribution, the grouping used consisted of the areas of Kiel Bay, Mecklenburg Bight, Arkona Sea, and Pomeranian Bight, while for analysis of the vertical distribution the samples were separated in SML, SSW, deep layer and the combination of SML and SSW. No linearity is assumed by using this ecological tool. The indicators provided by this analysis represent the DOM_{ISA}.

Statistical analyses were performed using R, version 2023.06.0. Descriptive statistics comprising medians and interquartile ranges were employed and evaluated with the Kruskal-test and Dunn-test (*rstatix* Package), assuming a 95 % confidence level. A maximum likelihood function tested model assumptions (normality, linearity, and residual homoscedasticity) (*boxcox*, MASS package, Venables and Ripley, 2002). The Spearman correlation (r_S) analysis assessed potential correlations between the analyzed parameters. Wind backwards trajectories were

calculated to demonstrate where the air masses passed before reaching the sampling areas seven days before sampling (Fig. S1; Meteorological Data Explorer (METEX) from the National Institute for Environmental Studies Global Environmental Database; https://db.cger.nies.go.jp/ged/metex/en/index.html) and plotted using the *openair* package in R (Carslaw and Ropkins, 2012). Non-metric multidimensional scaling (NMDS) was used to determine correlations of environmental variables with the DOM_{ISA}. The environmental variables were centered and scaled for ordination. All NMDS models were run on Bray–Curtis distance matrix, and their statistical significance was tested with 10,000 permutations (*vegan* package). Ocean Data View (version 5.6.5; Schlitzer, 2023) was used to produce surface plots of the distributions of PAH, DBC, AI_{MOD} and B6CA:B5CA ratio. Only the SSW (~1 m depth) data was used to generate the distribution surface plots.

3. Results

3.1. Field environmental parameters

Humidity, wind direction, and wind speed were considered in the data evaluation since they can interfere with the atmospheric transport of pollutants to the water (Table S1; Masiol et al., 2013; M. Zhao et al., 2013; X.J. Zhao et al., 2013), dilute or concentrate the PAH in the atmosphere (Wiriya et al., 2013; He et al., 2014), and influence the stability of the SML (Martinez-Varela et al., 2022). During the cruise, humidity ranged between 55 and 96 %, while wind direction and speed varied between 7.15 and 354.2° (median: 182.45°) and 0.9 and 14.7 m s $^{-1}$ (median: 7.4 m s $^{-1}$), respectively. Wind direction was characterized by a frequent easterly component, except during the sampling in the Pomeranian Bight, captured by the 7-day wind backwards trajectories (Fig. S1).

In the water column, PAH concentrations can be affected by parameters such as water temperature, salinity, and organic matter content (Table S1; Table S2; Huang et al., 2020). Water temperature varied between 5 and 8 $^{\circ}\text{C}$ (average: 5.7 \pm 0.65 $^{\circ}\text{C}),$ with higher temperatures in Kiel Bight when compared to the other areas and no statistical difference observed for the water layers (Kruskal-test, p < 0.001 and p =0.526, respectively). Salinity varied horizontally in the water column (between 6.35 and 20.63), with slightly higher salinity in the deep layer, and with values decreasing towards the Pomeranian Bight due to the Oder River discharge. Nitrite concentrations varied between 0.01 and $0.97~\mu M$ (average: $0.08~\pm~0.18~\mu M$), without significant vertical or horizontal differences in the study area. In comparison, nitrate concentrations ranged between 0.01 and 28.05 μM (average: 1.71 \pm 4.63 μM), with similar and low concentrations found in Kiel Bay, Mecklenburg Bight, and Arkona Sea (average: $0.75 \pm 1.04 \mu M$), and greater concentrations in the Pomeranian Bight, decreasing with increasing depth (Kruskal-test, p < 0.001). DOC and DON concentrations ranged from 161 to 337 μM (average: 270 \pm 34 $\mu M)$ and from 9 to 45 μM (average: 15 \pm 4 μ M), respectively. DOC concentrations decreased with increasing salinity in the SSW (DOC = 347–8.0; p < 0.001, $R^2 = 0.39$) and deep layer (DOC = 352–6.8; p < 0.001, $R^2 = 0.60$) while no trend was observed for the SML samples. The DOC concentrations differed between the areas with 243 \pm 40 $\mu M,$ 264 \pm 29 $\mu M,$ 294 \pm 22 $\mu M,$ and $308 \pm 24 \, \mu M$, in Kiel Bay, Mecklenburg Bight, Arkona Sea, and Pomeranian Bight, respectively.

3.2. Dissolved organic matter molecular-level composition

Ultrahigh-resolution mass spectrometric analysis of the solid-phase extractable DOM resulted in 6913 assigned MF over the whole dataset comprising 84 samples (Table S4), with most MF attributed to CHO and CHON groups, with 3000 and 2672 MF, respectively, accounting for 81 \pm 0.9 and 13 \pm 0.6 % of the relative intensity per sample. Indicator species analysis was used for the horizontal (Kiel Bay, Mecklenburg Bight, Arkona Sea, and Pomeranian Bight) and vertical (SML, SSW, and

deep layer) distribution, and out of the 6913 MF, 1486 MF (DOM_{ISA}) were associated to at least one of the areas (p < 0.1; Fig. 2A). From DOMISA, 665 MF were associated with Kiel Bight, 12 MF with Mecklenburg Bight, 218 MF to Arkona Sea, and 591 MF associated with Pomeranian Bight. In this subset, the CHO class of compounds represented high relative intensities in Mecklenburg Bight, Arkona Sea, and Pomeranian Bight, with 65 \pm 2.4, 98 \pm 0.2, and 91 \pm 0.2 %, respectively, while CHON compounds represented higher intensities in Kiel Bay, accounting for 66 \pm 1.7 % (Fig. 2A). Vertically, 368 MF were associated with the SML, 73 MF with the SSW, 33 MF were associated with both the SML and SSW, and 77 MF with the deep layer (Fig. 2B). The intensity-weighted contribution of the CHO class of compounds dominated in the DOMISA regarding water depth (analysis by water depth, vertical grouping), where the CHO compounds accounted for 53 \pm 4 % of the relative intensities, followed by the N-containing compounds with 30 \pm 4 %, and then by the CHOS class of compounds comprising 14 \pm 3 %.

3.3. Thermogenic organic matter and sources and imprint in DOM pool

The PAH concentrations in the Baltic Sea water column from the southwestern sampling area to the Pomeranian Bight (Fig. 3A and D; Table S3) ranged from 2.35 to 29.69 ng L $^{-1}$ (average: 16.05 \pm 4.44 ng L⁻¹, sum of 16 EPA-PAH) with a significant contribution of low molecular weight (LMW) PAH (average: $12.615 \pm 3.89 \text{ ng L}^{-1}$) compared to the high molecular weight (HMW) PAH (average: 3.44 \pm 1.02 ng L⁻¹). No difference in PAH concentrations was observed between the areas (Kruskal-test, p = 0.183; Fig. 3A). Still, Pomeranian Bight presented a slightly higher average (average: 18.62 ± 3.65 ng L⁻¹), followed by Arkona Sea (average: 16.74 ± 4.93 ng L⁻¹), Kiel Bay (average: 16.11 ± 2.35 ng L $^{-1}$) and Mecklenburg Bight (average: 15.44 ± 4.65 ng L⁻¹), with SSW concentrations elevated closer to the coastline east of Kiel Bay (Fig. 4A). 4-ring PAH were slightly higher in the Kiel Bay area, followed by Arkona Sea, Mecklenburg Bight, and Pomeranian Bight (Kruskal-test, p = 0.020), while 3-, 5- and 6-ring PAH concentrations were similar between the areas (Kruskal-test, p > 0.1). The most abundant HMW PAH were pyrene and fluoranthene, ranging from 61 to 73 % of the HMW PAH in the sampling areas, with pyrene concentrations decreasing towards the Pomeranian Bight area (Kruskal-test, p = 0.005). Naphthalene and fluorene concentrations slightly increased in the Pomeranian Bight samples (Kruskal-test, p=0.012 and p=0.023, respectively). Vertically, no difference in PAH concentrations was observed (Kruskal-test, p=0.367; Fig. 3D), with concentrations in the SML averaging at 17.81 \pm 1.40 ng L $^{-1}$, followed by SSW with a mean of 16.06 ± 0.73 ng L⁻¹ and deep layer with an average of 15.57 ± 0.73 ng L⁻¹. LMW and HMW PAH concentrations in the water column were similar (Kruskal-test, p > 0.210). In the SML, LMW and HMW PAH concentrations averaged at 15.52 \pm 1.23 ng L⁻¹ and 3.29 \pm 0.32 ng L⁻¹, respectively. In the SSW, the concentrations averaged at 12.40 \pm 0.64 ng $\ensuremath{\text{L}^{-1}}$ and 3.66 \pm 0.17 ng $\ensuremath{\text{L}^{-1}}$, respectively, while in the deep layer, the concentrations averaged at 12.31 \pm 0.64 ng L⁻¹ and 3.25 \pm 0.17 ng L⁻¹, respectively. 3-, 4-, 5- and 6-rings PAH had a similar vertical distribution in the water column (Kruskal-test, p > 0.1). The most abundant PAH in the samples was phenanthrene, followed by naphthalene. Fluoranthene had a slightly higher concentration in the SML, followed by SSW and deep layer, with averages of 0.89 \pm 0.07 ng L⁻¹, 0.87 \pm 0.04 ng L⁻¹, and 0.75 ± 0.04 ng L⁻¹, respectively (Kruskal-test, p > 0.1).

The BPCA method for DBC determination offers an alternative approach to measuring complex and larger polycyclic thermally modified organic matter structures than PAH (Table S5; Wiedemeier et al., 2015). DBC concentrations varied between 6.2 and 25.7 μ M (average: $14.2\pm2.8~\mu$ M) in the water column, with the B6CA:B5CA ratio varying between 0.30 and 0.36, with lowest surface water ratios in the eastern study area ratios. DBC accounted for $5.3\pm0.9~\%$ of DOC concentrations, varying between 2.1 and 8.6 % of DOC. PAH concentrations exhibited a different pattern than DBC concentrations in the SSW water in the area

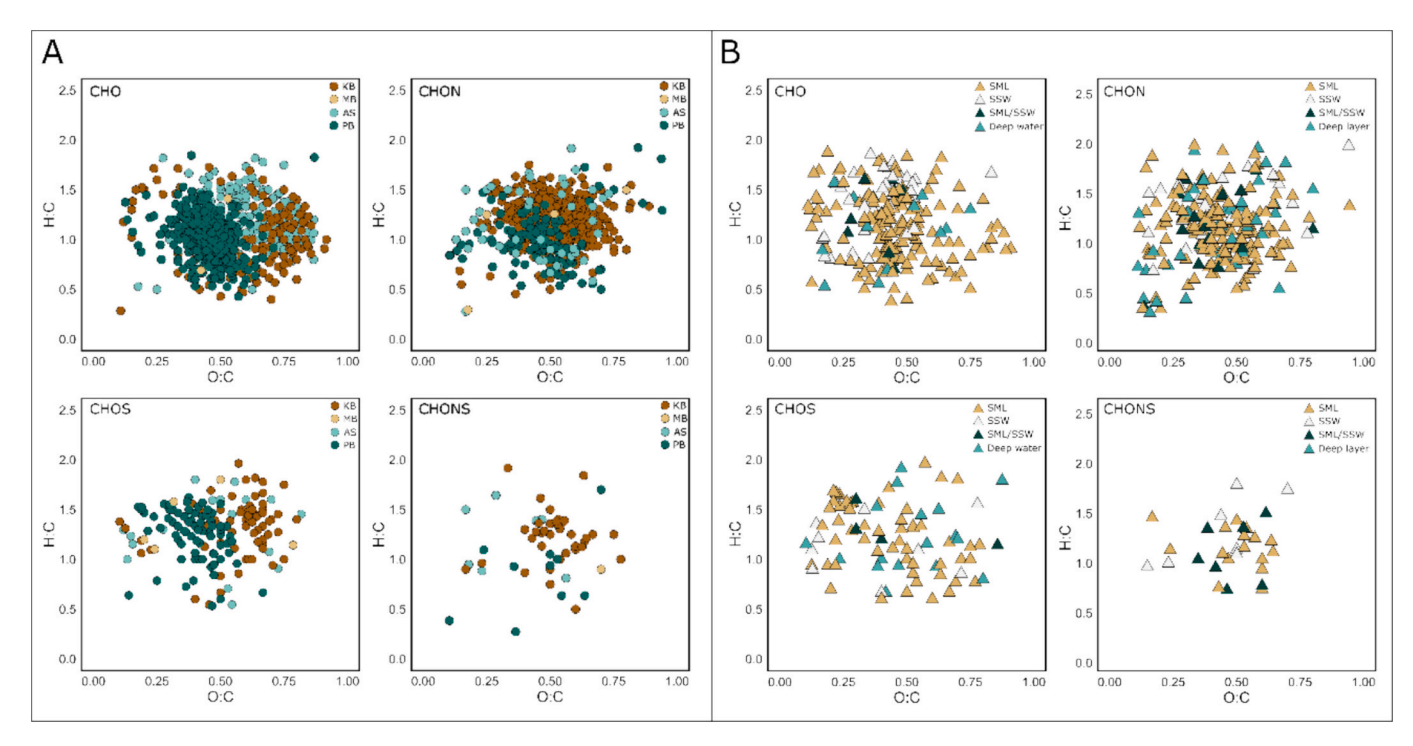


Fig. 2. Molecular formulae identified via Indicator Species Analysis associated with areas (Kiel Bay [KB], Mecklenburg Bight [MB], Arkona Sea [AS], and Pomeranian Bight [PB]) (A), and with the water column (SML, the SSW, the shared indicators between SML and SSW, and the deep layer) (B) by compound group represented in van Krevelen space.

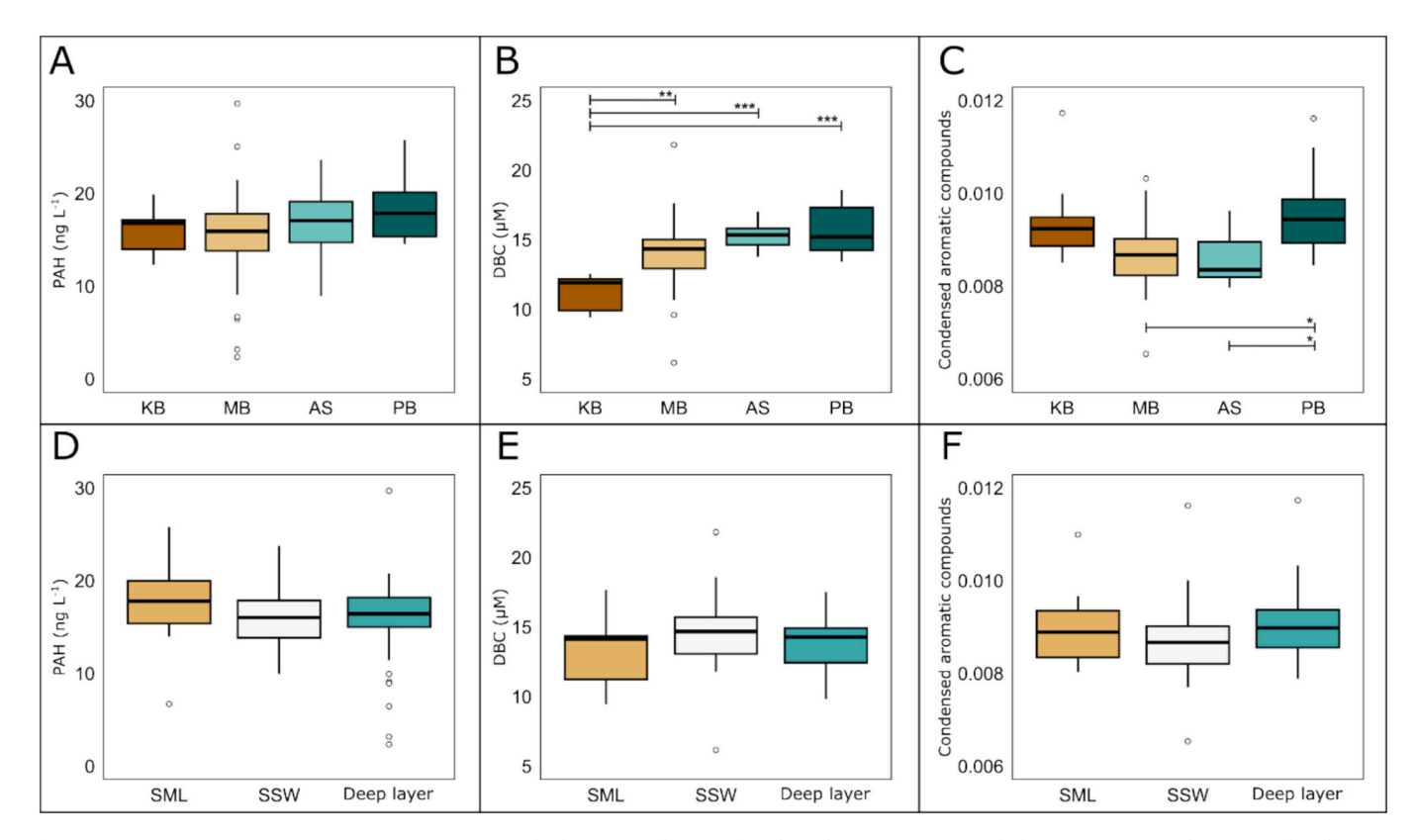


Fig. 3. PAH concentrations (A), DBC concentrations (B), and relative contribution of condensed aromatic compounds from FT-ICR-MS analysis (C) within the areas: Kiel Bay (KB), Mecklenburg Bight (MB), Arkona Sea (AS) and Pomeranian Bight (PB); PAH concentrations (D), DBC concentrations (E) and relative contribution of condensed aromatic compounds from FT-ICR-MS analysis (F) by water layer. *, **, *** indicate significance level of p < 0.05, p < 0.01, and p < 0.001 for the Dunntest, respectively.

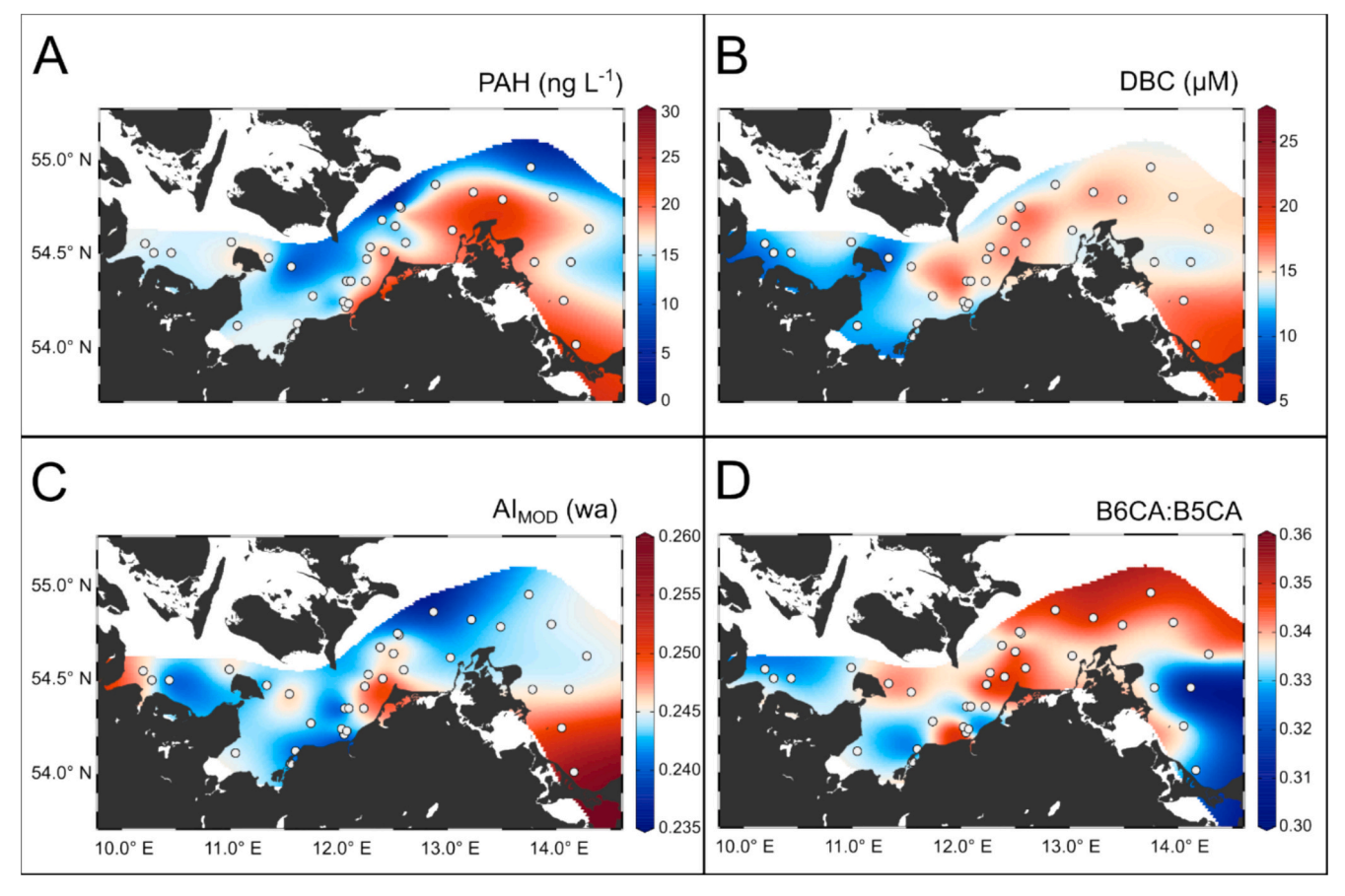


Fig. 4. Surface distribution of PAH concentrations (A), DBC concentrations (B), aromaticity index (AI_{MOD}) (C), and B6CA:B5CA ratios (D). Plotted with Ocean Data View using DIVA gridding interpolation (Schlitzer, 2023).

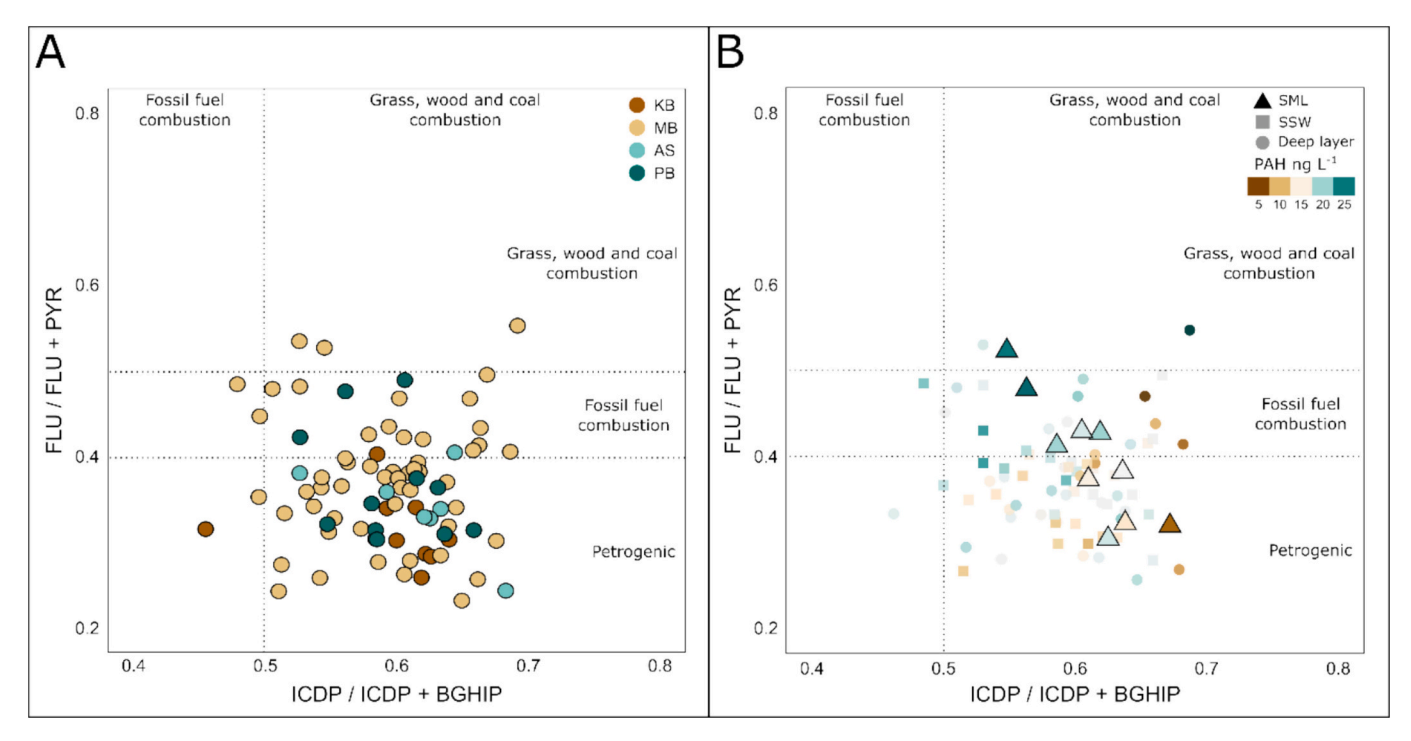


Fig. 5. PAH source apportionment from diagnostic ratios. Representation of data by areas, including Kiel Bay (KB), Mecklenburg Bight (MB), Arkona Sea (AS), and Pomeranian Bight (PB) (A), and within the water column, in the SML, SSW and deep layer with gradient of color representing PAH concentrations (B). Ratios are based on concentrations of indeno(1,2,3-c,d)pyrene (ICDP), fluoranthene (FLU), pyrene (PYR), and benzo(g,h,i)perylene (BGHIP).

(Fig. 4A and B, respectively). Horizontally, DBC content was higher in Pomeranian Bight (average: $15.7 \pm 1.8 \,\mu\text{M}$), Arkona Sea (average: $15.3 \pm 1.0 \,\mu\text{M}$), and Mecklenburg Bight (average: $14.0 \pm 3.3 \,\mu\text{M}$), with lower concentrations in Kiel Bay (average: $11.3 \pm 1.2 \,\mu\text{M}$) (Kruskal-test, p < 0.001), with slightly different B6CA:B5CA ratios in the SSW in the study area (Fig. 4D). Higher B6CA:B5CA ratios were observed in Arkona Sea (average: $0.34 \pm 0.01 \,\mu\text{M}$), and Mecklenburg Bight (average: $0.34 \pm 0.01 \,\mu\text{M}$) and Pomeranian Bight (average: $0.33 \pm 0.004 \,\mu\text{M}$) and Pomeranian Bight (average: $0.33 \pm 0.01 \,\mu\text{M}$) (Kruskal-test, p < 0.001). In the water column, DBC concentrations were similar in all layers (Kruskal-test, p = 0.291; Fig. 3E), while the B6CA:B5CA ratio was higher in the SSW (average: $0.34 \pm 0.01 \,\mu\text{M}$), followed by the SML and the deep layer (average: $0.33 \pm 0.01 \,\mu\text{M}$) (Kruskal-test, p = 0.018). The assigned condensed aromatic compounds in DOM_{ISA} showed a spatial variability with higher relative weighted intensities in Pomeranian Bight and Kiel

Bay, followed by Mecklenburg Bight and Arkona Sea (Kruskal-test, p = 0.002; Fig. 3C). In contrast, no pattern was observed over water depth (Kruskal-test, p = 0.152; Fig. 3F).

The apportionment of PAH sources was done by coupling diagnostic ratios, and the biplot shows that the sources varied between fossil fuel, biomass combustion, and petrogenic input in Kiel Bay, Mecklenburg Bight, Arkona Sea, and Pomeranian Bight (Fig. 5A), with PAH concentrations increasing in the SML with increasing contribution from biomass combustion (Fig. 5B). PAH concentrations were strongly negatively correlated with ICDP/ICDP+BGHIP ratio ($r_{\rm S}=-0.82,\,p=0.004$) and positively correlated with FLU/FLU+PYR ($r_{\rm S}=0.745,\,p=0.013$). No correlation was observed between the diagnostic ratios and environmental parameters such as geographical coordinates, DOC or nutrient concentrations.

The non-metric multidimensional scaling plots (Fig. 6) provide a

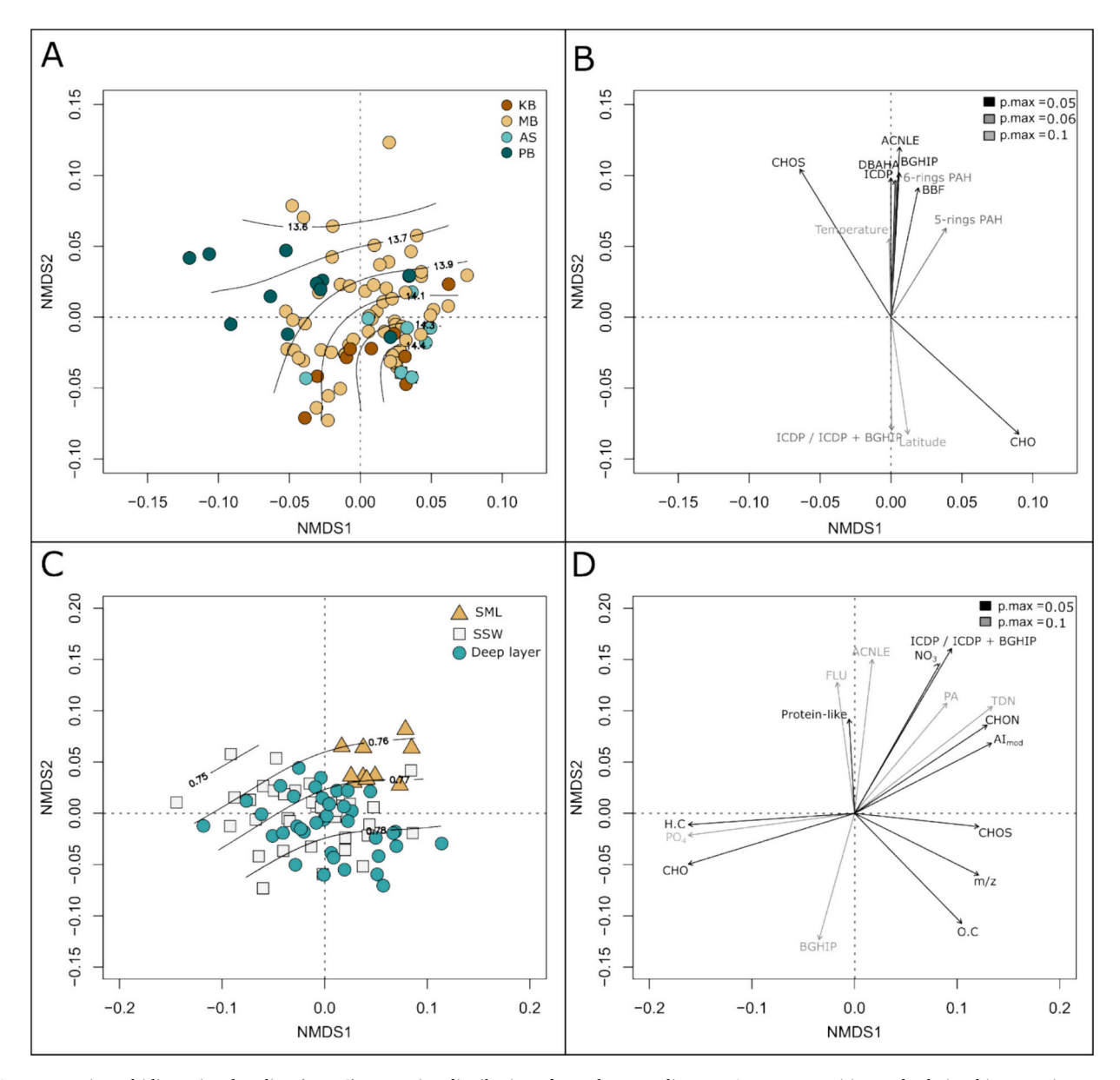


Fig. 6. Non-metric multidimensional scaling (NMDS) portraying distribution of samples according to DOM_{ISA} composition and relationship to environmental and combustion product parameters plus DOM characteristics. NMDS across areas including Kiel Bay (KB), Mecklenburg Bight (MB), Arkona Sea (AS), and Pomeranian Bight (PB) (A), and significantly related parameters (B). NMDS for DOM_{ISA} over the water column differentiating SML, SSW and deep layer (C) with related parameters (D); *m/z*: weighted average of molecular mass from FT-ICR-MS analysis, H.C: weighted average of hydrogen-to-carbon ratio, and O.C: weighted average of oxygen-to-carbon-ration from FT-ICR-MS analysis. Contours represent DBC concentrations and aromatic compounds that are likely derived from lignin degradation relative abundance (A and C, respectively).

multivariate view of DOM_{ISA} distribution from the southwestern Baltic Sea to the Pomeranian Bight area (Fig. 6A and B) as well as vertically within the water column (Fig. 6C and D). Key parameters covarying with the DOM_{ISA} are represented by the arrows, such as 5- and 6-rings PAH, and temperature for the areas (Fig. 6B) or phosphate, N- and S-containing compounds, and ICDP/ICDP+BGHIP for the water column (Fig. 6D).

4. Discussion

4.1. Dissolved organic carbon and nitrogen distributions

Water column characteristics revealed mixing of fresh- and saltwater as a major factor driving organic matter dynamics along the sampled stations from the southwestern Baltic Sea area to the Pomeranian Bight. Higher DOC concentrations in the Pomeranian Bight and decreasing linearly towards Kiel Bay while salinity increased, as previously observed by Seidel et al. (2017). The higher concentrations in Pomeranian Bight can be attributed to the contribution of allochthonous loading from the Oder River to the Baltic Sea and the subsequent enhanced autochthonous production (Nausch et al., 2008). Indeed, nitrate concentrations were higher in the Pomeranian Bight, exhibiting the same pattern as DOC concentrations. According to Beltran-Perez and Waniek (2022), the spring bloom occurs around day 85 \pm 7 (between 19 and 31st March), reaching the maximum biomass production on day 115 ± 6 (between 18 and 30 April), which can, along with the nutrient data presented here, indicate that the diatom bloom was already ongoing during the sampling period. The linear decrease of DOC observed from Pomeranian Bight to Kiel Bay can be attributed to the dilution of terrestrial input with the Baltic Sea water and removal of terrestrial DOC in the Baltic Sea water column, where around 56 % of terrestrial DOC is remineralized (Gustafsson et al., 2014). In spite of high turnover, Deutsch et al. (2012) reported a terrestrial contribution to the DOM in the area under the influence of the Oder River plume between 60 and 72 % and Seidel et al. (2017), by using the isotopic composition of carbon $(\delta^{13}C)$ as terrigenous OM tracer, also highlighted the importance of terrestrial input to the DOM pool of the Baltic Sea.

Recently, the agriculture and transport sectors were identified as the primary sources of nitrogen in the Baltic Sea (Gauss et al., 2021), with the contribution of TDN from ship sources horizontally homogeneously distributed in the upper 10 m of the water column (Neumann et al., 2020). With nutrient concentrations varying similarly vertically and horizontally in the study area, in the Pomeranian Bight, the concentrations of nitrite and phosphate were positively correlated with the terrestrial signature in DOM (ITERR index; Medeiros et al., 2016), inferring leaching of organic matter from soils and subsequent lateral transport into the aquatic systems. According to Neumann et al. (2020), the concentrations of bulk nitrogen from shipping emissions do not show a pattern in the western Baltic Sea due to the atmospheric transport and subsequent high atmospheric residence time of NO_X from shipping emission, which can explain the lack of relationship between nutrients and the distance from the shipping lanes in our study. With none of the nutrient concentrations increasing in the SML with respect to the proximity to the shipping routes nor enrichment in the layer with respect to SSW, nutrient distribution across the study areas can also be associated with the uptake dominated by diatoms during ongoing spring bloom, as depleted concentrations were observed for nitrate and silicate. Before the spring bloom, higher values for nitrate and phosphate were observed by Naumann et al. (2020) in surface water samples.

Overall, the mixing of freshwater from the Oder River with Baltic Sea water strongly influenced DOC and nutrient levels across the study area. Higher DOC and nutrient concentrations in the Pomeranian Bight, likely due to terrestrial inputs and resulting diatom blooms, gradually decreased towards Kiel Bay. The observed nutrient patterns reflect both land-based sources and biological uptake, highlighting the complex interactions shaping water column characteristics in this region.

4.2. DOM molecular composition

The concentration and composition of the DOM in the well-mixed water column in the southwestern Baltic Sea are driven by input from terrestrial material transported via the Oder River and autochthonous production. Different tools, such as ISA to identify MF that can be used as indicators for the areas or within the water column, elemental ratios and compound group distributions can be used to understand sources and fate of DOM in the Baltic Sea water. The MF indicative of the four areas: Kiel Bay, Mecklenburg Bight, Arkona Sea, and Pomeranian Bight, respectively identified using ISA, revealed a distinct distribution of compounds especially for Kiel Bay and Pomeranian Bight (Fig. 2A). Vertically, many MF assigned from DOMISA in the water column were associated with the SML (Fig. 2B), presenting a distinct grouping compared to the SSW and deep layers (Fig. 6C and D). Aromatic compounds that are likely derived from lignin degradation were abundant in the indicator MF for the Pomeranian Bight area, followed by Mecklenburg Bight, Arkona Sea, and Kiel Bay (Kruskal-test, p < 0.001). Ligninlike compounds were also abundant in the deep layer, followed by the SSW and SML (Kruskal-test, p = 0.003), while protein-like compounds were abundant in the SML, followed by SSW and deep layer (Kruskaltest, p = 0.0125). Lignin is a complex phenolic polymer present in terrestrial vascular plants tissues (Dittmar and Lara, 2001) commonly used as a terrestrial marker with a significant contribution of fluorescent moieties, and comprises much of the freshwater DOM transported to coastal seas, relatively enriching DOM with aromatic and complex compounds especially in the deep waters (Seidel et al., 2017; Li et al., 2020). Recently, lignin-like material was found to be abundant in humic-like substances in aerosols, reflecting local biomass burning or biofuel emissions (Sun et al., 2021). Protein-like compounds are surfaceactive compounds, and their higher contribution and accumulation in the SML can be expected due to its characteristics, e.g., surface tension reduced mixing, biological activities (Wurl et al., 2011). In addition, their presence was previously linked to biological production by phytoplankton communities as indicated by optical DOM analyses (Shields et al., 2019; Li et al., 2020), which can explain the strong positive correlation between protein-like compounds and TDN in the SML ($r_S = 0.68$, p = 0.029) and their link with SML DOM_{ISA} compounds (Fig. 6C and D).

CHO compounds were generally predominant in terms of number and relative abundance in all areas, except in Kiel Bay, where CHON compounds accounted for 66 ± 1.7 % of the overall relative intensity. Seidel et al. (2017) found that N-containing compounds were more abundant near Kattegat, and the authors attribute this to the marine influence in the area. CHON compounds in seawater can reflect autochthonous production or/and combustion products, with different numbers of nitrogen atoms indicating CHON transformations in aquatic environments along a salinity gradient (Yan et al., 2023, 2024). According to Yan et al. (2024), the lower the number of nitrogen atoms in the MF, the more saturated and less aromatic they are, with molecular transformations indicating DON degradation. S-containing groups are usually linked to the contribution of fossil fuel to DOM (Mead et al., 2013; Zhao et al., 2023), however, their relative contribution was low among the DOM $_{ISA}$ horizontally (4 \pm 0.3 %) and vertically (8 \pm 1 %) in the water column, and overall, no correlation was found with salinity or DOC. Nevertheless, NMDS analysis (Fig. 6A and B) indicated a clear association of S-containing groups with the samples from the Pomeranian Bight, suggesting local inputs, potentially influenced by riverine discharge and/or atmospheric deposition from Poland (Supplementary Fig. 1). Overall, complex interactions between terrestrial inputs and autochthonous production shape the composition of DOM in the southwestern Baltic Sea to Pomeranian Bight area. The distinct distribution of the compound groups across different areas and in the water column reveals the influence of both land-derived and marine processes. These findings underscore the importance of understanding both terrestrial and marine contributions to DOM, providing valuable insights

into the biogeochemical processes shaping the Baltic Sea.

4.3. Thermogenic organic matter distribution through different analytical windows

The untargeted and targeted approaches for thermogenic organic matter characterization revealed different patterns in the study area, emphasizing the mixing of prominent riverine inputs ultimately sourced from soils, atmospheric inputs on land, additional industrial and residential contributions to the rivers, plus atmospheric deposition directly to the Baltic Sea from shipping, road traffic, household and industrial point sources. Overall, anthropogenic sources such as the burning of fossil fuel and biomass contribute >60 % of the atmospheric BC, most of which eventually reaches the ocean (Yang et al., 2018). Both methods, PAH and DBC determination via BPCA quantification, are indicators for thermogenic/pyrogenic organic matter (Brodowski et al., 2005; Rodionov et al., 2010; Sánchez-García et al., 2010). PAH analysis quantifies specific molecules produced by high-temperature combustion with a critical ecological role due to their harmful characteristics. The BPCA method comprises PAH molecules, but can detect more complex aromatic thermogenic organic compounds and larger molecules than the targeted PAH analysis, offering a better understanding of the distribution of a wider range of thermogenic compounds in the environment (Hindersmann et al., 2020), but potentially also including highly condensed matter from non-pyrogenic sources (Kappenberg et al., 2016; Wagner et al., 2019). Combining these methods with known analytical windows in a multi-proxy approach can help to provide a more robust understanding of sources, transformations and distribution of thermogenic organic matter, mitigating interpretation biases. PAH concentrations were similar from Kiel Bay to the Pomeranian Bight throughout the water column, while DBC was strongly correlated to bulk DOC and decreased from Pomeranian Bight to Kiel Bay. DOC concentrations were positively correlated with DBC and weakly negatively correlated with PAH concentrations. Nevertheless, DBC was strongly negatively correlated with salinity ($r_S = -0.69$, p = 0.009), while PAH concentrations did not correlate with salinity ($r_S = -0.04$, p > 0.276). This suggests two different sources or paths for PAH and DBC, where DBC is mainly transported to the Baltic Sea by river, while PAH distribution in the brackish Baltic Sea is homogeneous despite riverine input. PAH distribution across the study area hence can be a result of several facts, such as partitioning between dissolved and particulate fractions, dilution effects from mixing processes, or photo- and/or biodegradation.

DBC concentrations in the Baltic Sea (ranging from 6.2 to 25.7 $\mu M_{\mbox{\tiny H}}$ averaging at 14.2 \pm 2.8 μ M) were higher than in other coastal systems, e.g., Chukchi Sea and Bering Sea (0.6 to 1.9 μM; Nakane et al., 2017), South China Sea (0.6 to 1.6 µM; Fang et al., 2017), Southeastern Brazil (0.3 and 17 μ M; Marques et al., 2017), East China Sea (0.7 and 1.9 μ M; H. Bao et al., 2023; M. Bao et al., 2023) and South Yellow Sea (0.97 and 1.7 μM; H. Bao et al., 2023; M. Bao et al., 2023). The high concentrations in the Baltic Sea reflect the persistent anthropogenic pressure, with landbased input to the semi-enclosed Baltic Sea and the local emissions from shipping or road traffic that due to the low water exchange with the North Sea, can remain in the Baltic Sea. No DBC data was previously reported from the Baltic Sea, although Ljung et al. (2022) analyzed the sedimentary BC content, showing an increase in concentrations starting in the 1940s, with biomass as the primary source as a consequence of emission from wood burning used for energy production, underpinning a likely at least partial contribution of direct anthropogenic emissions also to the Baltic Sea DBC. In addition to acting as a tracer for thermogenic inputs, BC comprises the longest-lived carbon fraction with average turnover times of \sim 40,000 yrs in the global ocean (Hansell, 2013) and millennia-scale stability in marine sediments (Masiello and Druffel, 1998), thereby rendering BC a candidate for carbon storage.

PAH concentration in the Pomeranian Bight was previously reported to result from land-based sources transported to the coastal sea via the Oder River's estuary (Kanwischer et al., 2020). Salinity (varying from

6.35 to 8.31) negatively correlated with PAH ($r_S = -0.47$, p = 0.145), and DBC concentrations ($r_S = -0.58$, p = 0.080) in the Pomeranian Bight, indicating that despite PAH concentrations appearing homogeneous overall in the brackish Baltic Sea, the negative correlation with salinity in the Pomeranian Bight reveals some riverine transport of thermogenic organic matter to the area. In addition, the lower B6CA: B5CA ratio found in the Pomeranian Bight can indicate that DBC already underwent processing such as photodegradation, which removes the more aromatic portions and facilitates subsequent biodegradation (Wagner et al., 2015; Nakane et al., 2017). DOC concentrations frequently correlate to DBC concentrations and B6CA:B5CA ratios in aquatic environments (Marques et al., 2017; Wagner et al., 2018; Barton et al., 2024), but this was not observed in the Pomeranian Bight. No correlation was found between DBC and DOC as well as DBC and B6CA: B5CA ratios, potentially indicating an input of ship/atmospheric emissions to the DBC in the area to the DBC coming from riverine transport.

In the Arkona Sea, the thermogenic organic matter land-based input is likely overprinted by the imprint from shipping/atmospheric emissions. 6-rings PAH were strongly negatively correlated to the DOC concentrations ($r_S = -0.92$, p = 0.001), and DBC did not correlate with DOC concentrations ($r_S = -0.02$, p = 0.957). While the strong negative correlation between DBC and salinity ($r_s = -0.69$, p = 0.009) highlighted riverine input as a dominant source of DBC in the Pomeranian Bight, in the Arkona Sea, however, the lack of correlation between DBC and DOC concentrations suggests that additional contributions, such as localized atmospheric deposition from ship emissions, may play a role. This decoupling of DBC from DOC further emphasizes the complexity of thermogenic organic matter inputs and their transformation processes in the Baltic Sea. According to Neumann et al. (2020), differently from the other basins, the shipping contribution in the Arkona Basin continuously increases starting at the beginning of the year until summer. The increase in thermogenic organic matter sourced from ship traffic added to the land-based source could explain the lack of correlation between DOC and DBC and higher B6CA:B5CA ratio in the area. As observed by Martinot et al. (2024), thermogenic organic matter from ships can become part to DBC. In the Arkona Sea and Pomeranian Bight, wind speed and direction are important in distributing HMW PAH, e.g., benz (a)pyrene, indeno(1,2,3-c,d)pyrene, dibenzo(a,h)anthracene, and benz (g,h,i)perylene. They were negatively correlated with wind speed and positively with wind direction with a stronger impact in Pomeranian Bight. Wind backwards trajectories showed that in Pomeranian Bight, the stations were influenced by eastern and southeastern winds that likely transported material mainly from Poland (Fig. S1). It is known that Poland emits high levels of PAH from different sources, e.g., the primary use of coal/wood combustion for residential heating during winter, fossil fuel combustion, and industrial activities (Wolska et al., 2003; Garrido et al., 2014; Gaffke et al., 2015), which can impact HMW PAH in the coastal sea either via atmospheric deposition or riverine transport. In contrast, wind characteristics did not reveal any pattern in relation to PAH concentrations in Mecklenburg Bight or Kiel Bay. PAH diagnostic ratios and B6CA:B5CA ratios reveal distinct thermogenic organic matter sources. In the Pomeranian Bight, terrestrial runoff plays a dominant role, while in the Arkona Sea, atmospheric emissions likely including shipping emissions leave a clear imprint. These findings demonstrate the value of multi-proxy approaches in differentiating between overlapping anthropogenic and natural inputs in complex environments like the Baltic Sea.

PAH concentrations in the surface water of Kiel Bay were reported to have decreased from 9.2 ng L $^{-1}$ from 1993 to 1998 (Witt and Matthäus, 2001) to 5.2 ng L $^{-1}$ between 2003 and 2017 (Kanwischer et al., 2020). During the spring of 2023, PAH concentrations in the surface water (SSW) detected in this study averaged 8.29 \pm 1.56 ng L $^{-1}$ (Figs. 3D and 4A), higher than the range reported for January 2023 of 3.7 to 1.0 ng L $^{-1}$ (Naumann et al., 2023). Kanwischer et al. (2020) observed an increasing trend in Kiel Bay and Pomeranian Bight in the dissolved fraction of the water. However, it is important to note the difference between the

sampling method, where the authors performed transect-type sampling instead of point sampling. Compared with the PAH concentrations reported by Witt (2002), where PAH concentrations were reported as a sum of the concentration found in the dissolved and particulate fractions of the water collected between 1992 and 1998, the values reported here are higher by around 25 %. The increase in PAH concentrations is directly related to anthropogenic pressure in the Baltic Sea, e.g., shipping (atmospheric emission or discharge of enriched contaminated water) and land-based emissions (Jalkanen et al., 2021).

Concentrations of thermogenic organic matter over water depths were similar for PAH and DBC approaches, with no enrichment in the SML. Witt (2002), in a first approach evaluating PAH concentrations and distribution in the SML, found higher values (sum of dissolved and particulate PAH) in the SML in Mecklenburg Bight, Arkona Sea, and the Baltic Proper. The values were 10-fold higher than the surface water (SSW here) and were directly correlated to the suspended particulate matter concentration in the water. The partitioning of PAH between dissolved and particulate matter can be explained by the hydrophobicity of PAH, where the partitioning towards the adsorption of PAH onto particles is favored (Cai et al., 2018; Chen et al., 2022). Other abiotic processes, e.g., photodegradation, volatilization, adsorption, or biotic transformation, can play an essential role in transferring PAH and DBC from the SML to the atmosphere or to the water column or remineralizing it, decreasing the concentration in the dissolved phase (Stubbins et al., 2012; Duran and Cravo-Laureau, 2016; González-Gaya et al., 2016; Nakane et al., 2017; Martinez-Varela et al., 2022). As mentioned previously, during the sampling campaign EMB315 in Spring 2023, the water column was well mixed, which for the present study may explain the similar concentrations found throughout the water column; in addition, it is reported that wind speeds above 4 m s⁻¹ can disturb the organic biofilm formed in the SML (Romano and Garabetian, 1996). Here, wind speed averaged at 4.8 \pm 2.8 m s⁻¹ during SML sampling, potentially facilitating the removal and redistribution of thermogenic organic matter from the SML to the water column.

Wind direction was positively correlated with several PAH in the SML, such as fluorene ($r_S = 0.685$, p = 0.029), benz(a)anthracene ($r_S = 0.029$) 0.78, p = 0.007), chrysene ($r_S = 0.63$, p = 0.048), benz(b)fluoranthene $(r_S = 0.55, p = 0.098)$ and benz(a)pyrene $(r_S = 0.78, p = 0.007)$, and with DBC concentrations ($r_S = 0.54$, p = 0.107) with increasing concentrations when wind was from E-NE directions; at the same time, no correlation was observed with the PAH in the SSW. DOC concentration negatively correlated to all PAH in the SML, and again, no correlation was observed in the SSW samples. This lacking association in the dissolved fraction could enhance PAH bioavailability, increasing the possibility of bioaccumulation (Moeckel et al., 2014). Wu et al. (2011) investigated PAH concentrations and distribution in the water column of the Western Taiwan Strait, China, and did not find a relationship between PAH and DOC concentration or salinity either. The authors attributed this result to the dominance of atmospheric deposition of PAH over riverine transport, having mixed sources with land-based characteristics.

4.4. Sources and processes for thermogenic organic matter

By coupling PAH diagnostic ratios, it is possible to apportion the different sources, e.g., petrogenic, biomass, or fossil fuel combustion, that emit the pollutant into the water column (Fig. 5; Tobiszewski and Namieśnik, 2012; Duran and Cravo-Laureau, 2016; Li et al., 2016; Kanwischer et al., 2020; Vaezzadeh et al., 2021). However, we note that PAH diagnostic ratios can have limitations across different environmental matrices due to environmental conditions and processes, thus, they must be interpreted carefully (Tobiszewski and Namieśnik, 2012). For example, individual PAH can be photodegraded at different rates during (riverine) transport, which can mislead the interpretation as their source signal might be altered as shown by Jacobs et al. (2008). Likewise, atmospheric PAH are transported in the vapour phase or on aerosol

particles, and undergo ageing processes before reaching the aquatic system where they are exposed to further adsorption, desorption and transformation processes, complicating their source apportionment in the dissolved fraction of the water (Tobiszewski and Namieśnik, 2012). For the present research, we used the ICDP/ICPD+BGHIP ratio coupled to FLU/FLU+PYR ratio, since those ratios are more conservative (e. g., not altered by photodegradation) when compared to other diagnostic ratios, and their apportionment compared to compound-specific δ^{13} C for tracing sources presented a similar result (Okuda et al., 2002; Tobiszewski and Namieśnik, 2012).

As mentioned in the previous section, even though the concentrations are similar across the study area, different sources appear to contribute to the thermogenic organic matter in the Baltic Sea water column, from shipping emissions to residential heating that initially disperse the PAH into the atmosphere before reaching the water column, and riverine transport (Hermansson et al., 2021; Ytreberg et al., 2022). With a higher contribution of LMW PAHs compared to HMW PAHs, it is important to note that LMW dominance often suggests a significant petrogenic source (Li et al., 2015). However, this interpretation remains uncertain here due to the absence of PAH analysis in the particulate fraction, where a portion of the HMW PAHs is likely adsorbed due to their low water solubility, high hydrophobicity, surface interaction, and partition coefficient (Wu et al., 2011). Mostly visible in the SML, the concentrations of PAH in the SML relate to the source of the polycyclic aromatic compounds, with contributions from wood/coal combustion increasing with PAH concentrations and wind direction playing an important role in this layer (Figs. 5B, 6C and D). Potentially, residential heating on land supplied large amounts of fresh, PAH-laden aerosol during the cold spell end of March 2023, contributing to the thermogenic organic matter in the dissolved fraction of the water.

Furthermore, the B6CA:B5CA ratio showed a decoupling of DBC between Pomeranian Bight and the other areas, which was not reflected in the concentrations. Nakane et al. (2017) observed that DBC concentrations had a similar trend as the degree of condensation when analyzing the DBC distribution in the salinity gradient from Chukchi Sea to the Subtropical North Pacific, where the higher the DBC concentration, the higher the degree of condensation. Here, while DBC from Pomeranian Bight has lower degree of condensation but higher concentrations, Arkona Sea presented higher B6CA:B5CA ratios, which decreased towards Kiel Bay. In Pomeranian Bight, DBC concentrations were strongly negatively correlated with the distance from Oder River $(r_S = -0.76, p = 0.010)$, whereas in the other areas, no pattern was observed. This may indicate that DBC in Pomeranian Bight originates from land-based sources, e.g., soil, soot deposition from residential heating, being reworked over long periods of time before release into the Baltic Sea which was reflected in the surface water distribution in the study area (Fig. 4B). Similarly, the B6CA:B5CA ratio of the DBC in streams located in Japan were generally lower compared to ratios from the water-soluble fraction extracted from atmospheric dust (Ding et al., 2015; Yamashita et al., 2021). In Arkona Sea, shipping sources, in addition to other atmospheric deposition from long range atmospheric transport from land-based fossil fuel burning, and transport from the Baltic Proper facilitated by wind direction could result in the contribution of soot-DBC to the area that is subsequently transported towards Kiel Bay, with B6CA:B5CA ratio decreasing during transport due to e.g., photodegradation (Figs. 4D and 6A; Stubbins et al., 2012; Marques et al., 2017) or preferential absorption of larger compounds to particulate matter (Nakane et al., 2017). Photodegradation and microbial transformation are critical in modifying the composition of thermogenic organic matter. For instance, the lower B6CA:B5CA ratios in the Pomeranian Bight suggest advanced photochemical processing that reduces aromaticity and facilitates biodegradation. Conversely, PAHs display more homogeneous distributions due to partitioning and dilution processes. Overall, thermogenic organic matter distribution from the southwestern Baltic Sea to the Pomeranian Bight is driven by several sources in close proximity mixed in the shallow waters, and different

tools can help to decipher these sources and their importance.

4.5. Anthropogenic imprint in the DOM pool

The thermogenic organic matter from ultrahigh-resolution mass spectrometry identified further potential combustion products outside the defined list of PAHs. Some of the DOMISA CHO compounds associated with the Pomeranian Bight have been reported in atmospheric humic-like substances during the winter season in other regions previously (Sun et al., 2021; H. Bao et al., 2023; M. Bao et al., 2023), e.g., derived from products of secondary wood combustion (C14H8O4, $C_{14}H_8O_5$, $C_{13}H_8O_5$, $C_{13}H_8O_6$), from flavonoids ($C_{15}H_{10}O_6$, $C_{15}H_8O_6$, and C₁₆H₁₂O₇), and phenol derivatives produced by the pyrolysis of lignin (C₁₈H₁₄O₆ and C₁₈H₁₄O₇). These MF were identified by H. Bao et al. (2023) and M. Bao et al. (2023) while analyzing the composition of humic-like substances in atmospheric aerosols, in the Yangtze River Delta, China. In the present study, the MF C₁₃H₈O₆ had a high relative intensity among the ${\rm DOM}_{\rm ISA}$ MF in the Pomeranian Bight area with DBE and AI_{MOD} values of 10 and 0.7, which suggests the presence of condensed aromatic compounds likely emitted from incomplete combustion during the heating season via atmospheric deposition or riverine transport via Oder River into the Pomeranian Bight water column. Furthermore, detected in heavy fuel oil engine samples and later found in water-soluble humic-like aerosol fraction (Cui et al., 2019; H. Bao et al., 2023; M. Bao et al., 2023), C10H6O8 compounds were associated with Kiel Bight in the present study. Certain MF associated with the SML, e.g., C₁₅H₁₀O₆ and C₁₂H₁₆O₄S, were previously identified in coal combustion products (Cui et al., 2019; H. Bao et al., 2023; M. Bao et al., 2023). While it is important to note that a single MF identification likely represents many different isomers and does not necessarily represent the same structures across different environments, these common identifications can provide a valuable parallel and starting point for future research.

The groups of N- and S-containing compounds are important components of the soluble fraction of aerosols, and due to anthropogenic pressure, there is an increase in their relative intensity in aerosols (Laskin et al., 2009) and marine DOM (Yan et al., 2023). Schmitt-Kopplin et al. (2011) observed an increase in N- and S-containing compounds in the aerosol samples compared to sea surface marine DOM and attributed this enhancement to the anthropogenic input either by ship exhaust or biomass burning. In the present study, wind direction and benz(a)pyrene concentration were strongly correlated with S-containing compounds in the SML ($r_S = 0.76$ and p = 0.011; $r_S = 0.65$, p = 0.042, respectively), indicating that S-containing compounds and benz(a)pyrene may share the transport path to the SML from a similar source. It is known that fossil fuel combustion releases more CHOS compounds, while biomass combustion is frequently related to the release of CHO and CHON compounds (Zhao et al., 2023). S-containing compounds corresponded to 8 \pm 1 % of the intensities DOM_{ISA} in the SML, while Ncontaining compounds comprised 26 \pm 1 % and CHO compounds 65 \pm 1 % accounting for relative intensity. The condensed aromatic compounds assigned from DOMISA were overall not correlated to PAH and DBC concentrations ($r_S = 0.06$; $r_S = 0.02$, respectively, p > 0.361) and similar within the water column. The anthropogenic imprint in the DOM_{ISA} pool suggests atmospheric deposition and riverine transport contribution, linked to incomplete combustion processes, such as biomass burning and fossil fuel emissions. The presence of these compounds in the SML and their correlation with environmental factors highlight the significant impact of anthropogenic activities on the Baltic Sea's DOM. The detection of aerosol-derived compounds linked to wood combustion and fossil fuel emissions underscores the importance of marginal seas as carbon sinks under increasing anthropogenic pressures. These findings highlight the Baltic Sea's dual role in long-term carbon storage and as a repository for thermogenic organic matter, emphasizing the need for continued monitoring of these systems.

5. Conclusion

By coupling targeted and untargeted approaches to investigate the thermogenic organic matter distribution and sources, this study reveals distinct spatial patterns in the southwestern Baltic Sea. The findings emphasize the significant influence of terrestrial inputs from the Oder River and autochthonous production on the distribution of DOC concentrations. The presence of specific MF is indicative of organic matter sources as well as anthropogenic pressure from combustion products to the Baltic Sea. PAH and DBC reflect the concentration and distribution of thermogenic organic matter of different origin and cycling on a small scale from Kiel Bay to Pomeranian Bight. Together, this comprehensive assessment reveals the strengths and weaknesses of different approaches to characterize the thermogenic organic matter in the environment for understanding natural and anthropogenic factors shaping organic matter composition in the Baltic Sea, with a focus on the long-lived portion of the carbon pool.

CRediT authorship contribution statement

Tassiana S.G. Serafim: Writing – review & editing, Writing – original draft, Visualization, Validation, Methodology, Investigation, Formal analysis, Data curation, Conceptualization. Detlef E. Schulz-Bull: Supervision, Funding acquisition. Christopher P. Rüger: Writing – review & editing, Resources. Thorsten Dittmar: Writing – review & editing, Methodology. Ralf Zimmermann: Writing – review & editing, Funding acquisition. Joanna J. Waniek: Writing – review & editing, Supervision. Helena Osterholz: Writing – review & editing, Supervision, Project administration, Funding acquisition, Conceptualization.

Declaration of competing interest

The authors declare that they have no known competing financial interests or personal relationships that could have appeared to influence the work reported in this paper.

Acknowledgment

This research is part of the PlumeBaSe project, which is co-funded by the German Research Foundation (DFG—471841824) and the Czech Science Foundation (GACR, 22-03426L). R/V Elisabeth Mann Borgese cruise EMB315 was funded by the Leibniz Institute for Baltic Sea Research Warnemünde (IOW). The authors also thank the German Research Foundation for funding the Bruker FT-ICR-MS (INST 264/56). T. S. G. Serafim is grateful to the EMB315 scientific party, Captain T. Henning, and the crew. Serafim also acknowledges the immense support of J. Jeschek (IOW) during the preparation for the cruise and sampling processing, as well as the nutrient determination done by L. Kreuzer (IOW). Serafim is also grateful to I. Ulber (ICBM) and H. Simon (ICBM) for support with the BPCA procedure and analysis, as well as the participation of S. Haude (ICBM) during the EMB315 cruise.

Appendix A. Supplementary data

Supplementary data to this article can be found online at https://doi. org/10.1016/j.scitotenv.2025.178537.

Data availability

Data will be made available on request.

References

- Bao, H., Niggemann, J., Du, M., Zhao, W., Huang, D., Yi, Y., Yang, J.Y.T., Dittmar, T., Kao, S.J., 2023a. Deciphering sources and processing of dissolved black carbon in coastal seas. Limnol. Oceanogr. 68, 2562–2575. https://doi.org/10.1002/lno.12442.
- Bao, M., Zhang, Y.-L., Cao, F., Hong, Y., Lin, Y.-C., Yu, M., Jiang, H., Cheng, Z., Xu, R., Yang, X., 2023b. Impact of fossil and non-fossil fuel sources on the molecular compositions of water-soluble humic-like substances in PM 2.5 at a suburban site of Yangtze River Delta, China. Atmos. Chem. Phys. 23, 8305–8324. https://doi.org/10.5194/acp-23-8305-2023.
- Barton, R., Richardson, C.M., Pae, E., Montalvo, M.S., Redmond, M., Zimmer, M.A., Wagner, S., 2024. Hydrology, rather than wildfire burn extent, determines post-fire organic and black carbon export from mountain rivers in central coastal California. Limnol. Oceanogr. Lett. 9, 70–80. https://doi.org/10.1002/lol2.10360.
- Beltran-Perez, O.D., Waniek, J.J., 2022. Inter-annual variability of spring and summer blooms in the Eastern Baltic Sea. Front. Mar. Sci. 9. https://doi.org/10.3389/ fmars.2022.928633.
- Bond, T.C., Doherty, S.J., Fahey, D.W., Forster, P.M., Berntsen, T., DeAngelo, B.J., Flanner, M.G., Ghan, S., Kärcher, B., Koch, D., Kinne, S., Kondo, Y., Quinn, P.K., Sarofim, M.C., Schultz, M.G., Schulz, M., Venkataraman, C., Zhang, H., Zhang, S., Bellouin, N., Guttikunda, S.K., Hopke, P.K., Jacobson, M.Z., Kaiser, J.W., Klimont, Z., Lohmann, U., Schwarz, J.P., Shindell, D., Storelvmo, T., Warren, S.G., Zender, C.S., 2013. Bounding the role of black carbon in the climate system: a scientific assessment. J. Geophys. Res. 118, 5380–5552. https://doi.org/10.1002/jgrd.50171.
- Bostick, K.W., Zimmerman, A.R., Wozniak, A.S., Mitra, S., Hatcher, P.G., 2018. Production and composition of pyrogenic dissolved organic matter from a logical series of laboratory-generated chars. Front. Earth Sci. 6, 43. https://doi.org/ 10.3389/feart.2018.00043.
- Brodowski, S., Rodionov, A., Haumaier, L., Glaser, B., Amelung, W., 2005. Revised black carbon assessment using benzene polycarboxylic acids. Org. Geochem. 36, 1299–1310. https://doi.org/10.1016/j.orggeochem.2005.03.011.
- Cai, M., Duan, M., Guo, J., Liu, M., Qi, A., Lin, Y., Liang, J., 2018. PAHs in the Northern South China Sea: horizontal transport and downward export on the continental shelf. Mar. Chem. 202, 121–129. https://doi.org/10.1016/j.marchem.2018.03.004.
- Carslaw, D.C., Ropkins, K., 2012. openair an R package for air quality data analysis. Environ. Model Softw. 27–28 (0), 52–61. ISSN 1364-8152,. https://doi.org/10.10 16/j.envsoft.2011.09.008.
- Chen, Q., Ma, Y., Dong, J., Kong, Y., Wu, M., 2022. The chemical structure characteristics of dissolved black carbon and their binding with phenanthrene. Chemosphere 291, 132747. https://doi.org/10.1016/j.chemosphere.2021.132747.
- 132747. https://doi.org/10.1016/j.chemosphere.2021.132747.

 Coppola, A.I., Wiedemeier, D.B., Galy, V., Haghipour, N., Hanke, U.M., Nascimento, G.S., Usman, M., Blattmann, T.M., Reisser, M., Freymond, C.V., Zhao, M., Voss, B., Wacker, L., Schefuß, E., Peucker-Ehrenbrink, B., Abiven, S., Schmidt, M.W.I., Eglinton, T.I., 2018. Global-scale evidence for the refractory nature of riverine black carbon. Nat. Geosci. 11, 584–588. https://doi.org/10.1038/s41561-018-0159-8.
- Coppola, A.I., Seidel, M., Ward, N.D., Viviroli, D., Nascimento, G.S., Haghipour, N., Revels, B.N., Abiven, S., Jones, M.W., Richey, J.E., Eglinton, T.I., 2019. Marked isotopic variability within and between the Amazon River and marine dissolved black carbon pools. Nat. Commun. 10 (1), 4018. https://doi.org/10.1038/s41467-019-11543-9
- Cui, M., Li, C., Chen, Y., Zhang, F., Li, J., Jiang, B., Mo, Y., Li, J., Yan, C., Zheng, M., Xie, Z., Zhang, G., Zheng, J., 2019. Molecular characterization of polar organic aerosol constituents in off-road engine emissions using Fourier transform ion cyclotron resonance mass spectrometry (FT-ICR MS): implications for source apportionment. Atmos. Chem. Phys. 19, 13945–13956. https://doi.org/10.5194/acp.19.13945-2019
- Cunliffe, M., Wurl, O., 2014. Guide to best practices to study the ocean's surface. In: Occasional Publications of the Marine Biological Association of the United Kingdom. Marine Biological Association of the United Kingdom for SCOR, Plymouth, UK. https://doi.org/10.25607/OBP-1512, 118pp.
- Deutsch, B., Alling, V., Humborg, C., Korth, F., Mörth, C.M., 2012. Tracing inputs of terrestrial high molecular weight dissolved organic matter within the Baltic Sea Ecosystem. Biogeosci. Discuss. 9, 4483–4512. https://doi.org/10.5194/bgd-9-4483-2012.
- Ding, Y., Yamashita, Y., Jones, J., Jaffé, R., 2015. Dissolved black carbon in boreal forest and glacial rivers of central Alaska: assessment of biomass burning versus anthropogenic sources. Biogeochemistry 123, 15–25. https://doi.org/10.1007/ s10533-014-0050-7.
- Dittmar, T., 2008. The molecular level determination of black carbon in marine dissolved organic matter. Org. Geochem. 39, 396–407. https://doi.org/10.1016/j. orggeochem.2008.01.015.
- Dittmar, T., Koch, B.P., 2006. Thermogenic organic matter dissolved in the abyssal ocean. Mar. Chem. 102, 208–217. https://doi.org/10.1016/j.marchem.2006.04.003.
- Dittmar, T., Lara, R.J., 2001. Molecular evidence for lignin degradation in sulfate-reducing mangrove sediments (Amazônia, Brazil). Geochim. Cosmochim. Acta 65, 1417–1428. https://doi.org/10.1016/S0016-7037(00)00619-0.
- Dittmar, T., Koch, B., Hertkorn, N., Kattner, G., 2008. A simple and efficient method for the solid-phase extraction of dissolved organic matter (SPE-DOM) from seawater. Limnol. Oceanogr. Methods 6, 230–235. https://doi.org/10.4319/lom.2008.6.230.
- Dittmar, T., de Rezende, C.E., Manecki, M., Niggemann, J., Coelho Ovalle, A.R., Stubbins, A., Bernardes, M.C., 2012. Continuous flux of dissolved black carbon from a vanished tropical forest biome. Nat. Geosci. 5, 618–622. https://doi.org/10.1038/ngeo1541.
- Downham, R.P., Gannon, B., Lozano, D.C.P., Jones, H.E., Vane, C.H., Barrow, M.P., 2024. Tracking the history of polycyclic aromatic compounds in London through a River

- Thames sediment core and ultrahigh resolution mass spectrometry. J. Hazard. Mater. 473, 134605, https://doi.org/10.1016/j.jhazmat.2024.134605.
- Duran, R., Cravo-Laureau, C., 2016. Role of environmental factors and microorganisms in determining the fate of polycyclic aromatic hydrocarbons in the marine environment. FEMS Microbiol. Rev. 40, 814–830. https://doi.org/10.1093/femsre/ fuw031.
- Fang, Y., Chen, Y., Huang, G., Hu, L., Tian, C., Xie, J., Lin, J., Lin, T., 2021. Particulate and dissolved black carbon in coastal China seas: spatiotemporal variations, dynamics, and potential implications. Environ. Sci. Technol. 55, 788–796. https://doi.org/10.1021/acs.est.0c06386.
- Fang, Z., Yang, W., Chen, M., Ma, H., 2017. Source and fate of dissolved black carbon in the western South China Sea during the Southwest Monsoon prevailing season. J. Geophys. Res. https://doi.org/10.1002/2017JG004014.
- Feistel, R., Nausch, G., Wasmund, N., 2008. State and Evolution of the Baltic Sea, 1952–2005: A Detailed 50-year Survey of Meteorology and Climate, Physics, Chemistry, Biology, and Marine Environment. John Wiley & Sons.
- Gaffke, J., Lewandowska, A., Bartkowski, K., 2015. Polycyclic Aromatic Hydrocarbons (PAHs) in the atmosphere of the Baltic Sea Region. ECOCYCLES 1, 51–55. https://doi.org/10.19040/ecocycles.v1i2.44.
- Garrido, A., Jiménez-Guerrero, P., Ratola, N., 2014. Levels, trends and health concerns of atmospheric PAHs in Europe. Atmos. Environ. 99, 474–484. https://doi.org/10.1016/j.atmosenv.2014.10.011.
- Gauss, M., Bartnicki, J., Jalkanen, J.-P., Nyiri, A., Klein, H., Fagerli, H., Klimont, Z., 2021. Airborne nitrogen deposition to the Baltic Sea: past trends, source allocation and future projections. Atmos. Environ. 253, 118377. https://doi.org/10.1016/j. atmoseny.2021.118377.
- Glaser, B., Amelung, W., 2003. Pyrogenic carbon in native grassland soils along a climosequence in North America. Glob. Biogeochem. Cycles. https://doi.org/ 10.1029/2002GR002019
- González-Gaya, B., Fernández-Pinos, M.-C., Morales, L., Méjanelle, L., Abad, E., Piña, B., Duarte, C.M., Jiménez, B., Dachs, J., 2016. High atmosphere-ocean exchange of semivolatile aromatic hydrocarbons. Nat. Geosci. 9, 438–442. https://doi.org/ 10.1038/ngeo2714.
- Guitart, C., García-Flor, N., Dachs, J., Bayona, J.M., Albaigés, J., 2004. Evaluation of sampling devices for the determination of polycyclic aromatic hydrocarbons in surface microlayer coastal waters. Mar. Pollut. Bull. 48, 961–968. https://doi.org/ 10.1016/j.marpolbul.2003.12.002.
- Guitart, C., García-Flor, N., Bayona, J.M., Albaigés, J., 2007. Occurrence and fate of polycyclic aromatic hydrocarbons in the coastal surface microlayer. Mar. Pollut. Bull. 54, 186–194. https://doi.org/10.1016/j.marpolbul.2006.10.008.
- Gustafsson, B.G., Schenk, F., Blenckner, T., Eilola, K., Meier, H.E.M., Müller-Karulis, B., Neumann, T., Ruoho-Airola, T., Savchuk, O.P., Zorita, E., 2012. Reconstructing the development of Baltic Sea eutrophication 1850–2006. Ambio 41, 534–548. https:// doi.org/10.1007/s13280-012-0318-x.
- Gustafsson, E., Deutsch, B., Gustafsson, B.G., Humborg, C., Mörth, C.-M., 2014. Carbon cycling in the Baltic Sea the fate of allochthonous organic carbon and its impact on air-sea CO2 exchange. J. Mar. Syst. 129, 289–302. https://doi.org/10.1016/j.imarsvs.2013.07.005
- Hansell, D.A., 2013. Recalcitrant dissolved organic carbon fractions. Annu. Rev. Mar. Sci. 5 (1), 421–445. https://doi.org/10.1146/annurev-marine-120710-100757.
- Harvey, G.W., Burzell, L.A., 1972. A simple microlayer method for small samples1. Limnol. Oceanogr. 17, 156–157. https://doi.org/10.4319/lo.1972.17.1.0156.
- He, J., Fan, S., Meng, Q., Sun, Y., Zhang, J., Zu, F., 2014. Polycyclic aromatic hydrocarbons (PAHs) associated with fine particulate matters in Nanjing, China: distributions, sources and meteorological influences. Atmos. Environ. 89, 207–215. https://doi.org/10.1016/j.atmosenv.2014.02.042.
- HELCOM, 2018. Baltic Marine Environment Protection Commission State of the Baltic Sea – Second HELCOM Holistic Assessment 2011–2016. Balt. Sea Environ. Proc. ISSN: 0357-2994 155.
- HELCOM, 2021. HELCOM AIS shipping density maps. https://metadata.helcom.fi/ge onetwork/srv/api/records/2558244b-0cea-46e9-8053-af6ef5d01853. (Accessed 25 March 2024).
- Hermansson, A., Hassellöv, I.-M., Moldanová, J., Ytreberg, E., 2021. Comparing emissions of polyaromatic hydrocarbons and metals from marine fuels and scrubbers. Transp. Res. D Trans. Environ. 97, 102912. https://doi.org/10.1016/j. trd/2021.102912
- Hindersmann, B., Förster, A., Achten, C., 2020. Novel and specific source identification of PAH in urban soils: Alk-PAH-BPCA index and "V"-shape distribution pattern. Environ. Pollut. 257, 113594. https://doi.org/10.1016/j.envpol.2019.113594.
- Huang, Y.J., Lin, B.S., Lee, C.L., Brimblecombe, P., 2020. Enrichment behavior of contemporary PAHs and legacy PCBs at the sea-surface microlayer in harbor water. Chemosphere 245, 125647. https://doi.org/10.1016/j.chemosphere.2019.125647.
- Jacobs, L.E., Weavers, L.K., Chin, Y.P., 2008. Direct and indirect photolysis of polycyclic aromatic hydrocarbons in nitrate-rich surface waters. Environ. Toxicol. Chem. 27 (8), 1643–1648. https://doi.org/10.1897/07-478.1.
- Jalkanen, J.-P., Johansson, L., Wilewska-Bien, M., Granhag, L., Ytreberg, E., Eriksson, K. M., Yngsell, D., Hassellöv, I.-M., Magnusson, K., Raudsepp, U., Maljutenko, I., Winnes, H., Moldanova, J., 2021. Modelling of discharges from Baltic Sea shipping. Ocean Sci. 17, 699–728. https://doi.org/10.5194/os-17-699-2021.
- Kanwischer, M., Bunke, D., Leipe, T., Moros, M., Schulz-Bull, D.E., 2020. Polycyclic aromatic hydrocarbons in the Baltic Sea - pre-industrial and industrial developments as well as current status. Mar. Pollut. Bull. 160, 111526. https://doi.org/10.1016/j. marpolbul.2020.111526.
- Kanwischer, M., Asker, N., Wernersson, A.-S., Wirth, M.A., Fisch, K., Dahlgren, E., Osterholz, H., Habedank, F., Naumann, M., Mannio, J., Schulz-Bull, D.E., 2022. Substances of emerging concern in Baltic Sea water: review on methodological

- advances for the environmental assessment and proposal for future monitoring. Ambio 51, 1588–1608. https://doi.org/10.1007/s13280-021-01627-6.
- Kappenberg, A., Bläsing, M., Lehndorff, E., Amelung, W., 2016. Black carbon assessment using benzene polycarboxylic acids: limitations for organic-rich matrices. Org. Geochem. 94, 47–51. https://doi.org/10.1016/j.orggeochem.2016.01.009.
- Koch, B.P., Dittmar, T., 2006. From mass to structure: an aromaticity index for high-resolution mass data of natural organic matter. Rapid Commun. Mass Spectrom. 20, 926–932. https://doi.org/10.1002/rcm.2386.
- Kuss, J., Nausch, G., Engelke, C., von Weber, M., Lutterbeck, H., Naumann, M., Waniek, J.J., Schulz-Bull, D.E., 2020. Changes of nutrient concentrations in the Western Baltic Sea in the transition between inner coastal waters and the central basins: time series from 1995 to 2016 with source analysis. Front. Earth Sci. China 8. https://doi.org/10.3389/feart.2020.00106.
- Laskin, A., Smith, J.S., Laskin, J., 2009. Molecular characterization of nitrogencontaining organic compounds in biomass burning aerosols using high-resolution mass spectrometry. Environ. Sci. Technol. 43, 3764–3771. https://doi.org/10.1021/ es803456n.
- Li, M., Xie, W., Li, P., Yin, K., Zhang, C., 2020. Establishing a terrestrial proxy based on fluorescent dissolved organic matter from sediment pore waters in the East China Sea. Water Res. 182, 116005. https://doi.org/10.1016/j.watres.2020.116005.
- Li, P., Cao, J., Diao, X., Wang, B., Zhou, H., Han, Q., Zheng, P., Li, Y., 2015. Spatial distribution, sources and ecological risk assessment of polycyclic aromatic hydrocarbons in surface seawater from Yangpu Bay, China. Mar. Pollut. Bull. 93, 53–60. https://doi.org/10.1016/j.marpolbul.2015.02.015.
- Li, X., Hou, L., Li, Y., Liu, M., Lin, X., Cheng, L., 2016. Polycyclic aromatic hydrocarbons and black carbon in intertidal sediments of China coastal zones: concentration, ecological risk, source and their relationship. Sci. Total Environ. 566-567, 1387–1397. https://doi.org/10.1016/j.scitotenv.2016.05.212.
- Lim, L., Wurl, O., Karuppiah, S., Obbard, J.P., 2007. Atmospheric wet deposition of PAHs to the sea-surface microlayer. Mar. Pollut. Bull. 54, 1212–1219. https://doi.org/ 10.1016/j.marpolbul.2007.03.023.
- Lima, A.L.C., Farrington, J.W., Reddy, C.M., 2005. Combustion-derived polycyclic aromatic hydrocarbons in the environment—a review. Environ. Forensic 6, 109–131. https://doi.org/10.1080/15275920590952739.
- Ljung, K., Schoon, P.L., Rudolf, M., Charrieau, L.M., Ni, S., Filipsson, H.L., 2022. Recent increased loading of carbonaceous pollution from biomass burning in the Baltic Sea. ACS Omega 7, 35102–35108. https://doi.org/10.1021/acsomega.2c04009.
- Manodori, L., Gambaro, A., Piazza, R., Ferrari, S., Stortini, A.M., Moret, I., Capodaglio, G., 2006. PCBs and PAHs in sea-surface microlayer and sub-surface water samples of the Venice Lagoon (Italy). Mar. Pollut. Bull. 52, 184–192. https://doi.org/10.1016/j.marpolbul.2005.08.017.
- Mari, X., Chu Van, T., Guinot, B., Brune, J., Lefebvre, J.-P., Raimbault, P., Dittmar, T., Niggemann, J., 2017. Seasonal dynamics of atmospheric and river inputs of black carbon, and impacts on biogeochemical cycles in Halong Bay, Vietnam. Elem. Sci. Anth. 5. 75. https://doi.org/10.1525/elementa.255.
- Marques, J.S.J., Dittmar, T., Niggemann, J., Almeida, M.G., Gomez-Saez, G.V., Rezende, C.E., 2017. Dissolved black carbon in the headwaters-to-ocean continuum of Paraíba Do Sul River, Brazil. Front. Earth Sci. Chin. 5. https://doi.org/10.3389/ feart.2017.00011.
- Martinez-Varela, A., Casas, G., Berrojalbiz, N., Piña, B., Dachs, J., Vila-Costa, M., 2022. Polycyclic aromatic hydrocarbon degradation in the sea-surface microlayer at coastal Antarctica. Front. Microbiol. 13, 907265. https://doi.org/10.3389/ fmich. 2022.907265
- Martinot, P.L., Guigue, C., Guyomarc'h, L., Mari, X., Chu, N.H., Vu, C.T., Boettcher, L., Dang, T.H., Niggemann, J., Dittmar, T., Tedetti, M., 2024 Sep 1. Optical characterization of black carbon-derived DOM: implication for the fluorescence detection of fuel combustion products in marine waters. Mar. Chem. 265, 104432. https://doi.org/10.1016/j.marchem.2024.104432.
- Masiello, C.A., Druffel, E.R., 1998 Jun 19. Black carbon in deep-sea sediments. Science 280 (5371), 1911–1913. https://doi.org/10.1126/science.280.5371.1911.
- Masiol, M., Formenton, G., Pasqualetto, A., Pavoni, B., 2013. Seasonal trends and spatial variations of PM10-bounded polycyclic aromatic hydrocarbons in Veneto Region, Northeast Italy. Atmos. Environ. 79, 811–821. https://doi.org/10.1016/j. atmoseny. 2013.07.025
- Mead, R.N., Mullaugh, K.M., Brooks Avery, G., Kieber, R.J., Willey, J.D., Podgorski, D.C., 2013. Insights into dissolved organic matter complexity in rainwater from continental and coastal storms by ultrahigh resolution Fourier transform ion cyclotron resonance mass spectrometry. Atmos. Chem. Phys. 13, 4829–4838. https://doi.org/ 10.5194/acp-13-4829-2013.
- Medeiros, P.M., Seidel, M., Niggemann, J., Spencer, R.G.M., Hernes, P.J., Yager, P.L., Miller, W.L., Dittmar, T., Hansell, D.A., 2016. A novel molecular approach for tracing terrigenous dissolved organic matter into the deep ocean. Glob. Biogeochem. Cycles 30, 689–699. https://doi.org/10.1002/2015gb005320.
- Meier, H.E.M., Eilola, K., Almroth-Rosell, E., Schimanke, S., Kniebusch, M., Höglund, A., Pemberton, P., Liu, Y., Väli, G., Saraiva, S., 2019. Disentangling the impact of nutrient load and climate changes on Baltic Sea hypoxia and eutrophication since 1850. Clim. Dyn. 53, 1145–1166. https://doi.org/10.1007/s00382-018-4296-y.
- Merder, J., Freund, J.A., Feudel, U., Hansen, C.T., Hawkes, J.A., Jacob, B., Klaproth, K., Niggemann, J., Noriega-Ortega, B.E., Osterholz, H., Rossel, P.E., Seidel, M., Singer, G., Stubbins, A., Waska, H., Dittmar, T., 2020. ICBM-OCEAN: processing ultrahigh-resolution mass spectrometry data of complex molecular mixtures. Anal. Chem. 92, 6832–6838. https://doi.org/10.1021/acs.analchem.9b05659.
- Meteorological Data Explorer (METEX), National Institute for Environmental Studies Global Environmental Database website. https://db.cger.nies.go.jp/ged/metex/en/index.html.

- Moeckel, C., Monteith, D.T., Llewellyn, N.R., Henrys, P.A., Pereira, M.G., 2014. Relationship between the concentrations of dissolved organic matter and polycyclic aromatic hydrocarbons in a typical U.K. upland stream. Environ. Sci. Technol. 48, 130–138. https://doi.org/10.1021/es403707q.
- Nakane, M., Ajioka, T., Yamashita, Y., 2017. Distribution and sources of dissolved black carbon in surface waters of the Chukchi Sea, Bering Sea, and the North Pacific Ocean. Front. Earth Sci. China 5. https://doi.org/10.3389/feart.2017.00034.
- Narloch, I., Gackowska, A., Wejnerowska, G., 2022. Microplastic in the Baltic Sea: a review of distribution processes, sources, analysis methods and regulatory policies. Environ. Pollut. 315, 120453. https://doi.org/10.1016/j.envpol.2022.120453.
- Naumann, M., Gräwe, U., Mohrholz, V., Kuss, J., Kanwischer, M., Feistel, S., Hand, I., Waniek, J.J., Schulz-Bull, D.E., 2020. Hydrographic-hydrochemical assessment of the Baltic Sea 2019. Meereswiss. Ber. Warnemünde 114. https://doi.org/10.12754/ msr-2020-0114.
- Naumann, M., Gräwe, U., Mohrholz, V., Kuss, J., Kanwischer, M., Osterholz, H., Feistel, S., Hand, I., Waniek, J.J., Schulz-Bull, D.E., 2023. Hydrographichydrochemical assessment of the Baltic Sea 2021. Meereswiss. Ber. Warnemünde 123. https://doi.org/10.12754/msr-2023-0123.
- Nausch, G., Nehring, D., Nagel, K., 2008. Nutrient concentrations, trends and their relation to eutrophication. In: State and Evolution of the Baltic Sea, 1952–2005. John Wiley & Sons, Inc., Hoboken, NJ, USA, pp. 337–366. https://doi.org/10.1002/ 9780470283134.ch12.
- Neumann, D., Karl, M., Radtke, H., Matthias, V., Friedland, R., Neumann, T., 2020. Quantifying the contribution of shipping NOx emissions to the marine nitrogen inventory – a case study for the western Baltic Sea. Ocean Sci. 16, 115–134. https://doi.org/10.5194/os-16-115-2020.
- Okuda, T., Kumata, H., Zakaria, M., Naraoka, H., Ishiwatari, R., Takada, H., 2002. Source identification of Malaysian atmospheric polycyclic aromatic hydrocarbons nearby forest fires using molecular and isotopic compositions. Atmos. Environ. 36, 611–618. https://doi.org/10.1016/S1352-2310(01)00506-4.
- Pradeep Ram, A.S., Mari, X., Brune, J., Torréton, J.P., Chu Van, T., Raimbault, P., Niggemann, J., Sime-Ngando, T., 2018. Bacterial-viral interactions in the sea surface microlayer of a black carbon-dominated tropical coastal ecosystem (Halong Bay, Vietnam). Elem. Sci. Anth. 6, 13. https://doi.org/10.1525/elementa.276.
- Riedel, T., Biester, H., Dittmar, T., 2012. Molecular fractionation of dissolved organic matter with metal salts. Environ. Sci. Technol. 46, 4419–4426. https://doi.org/ 10.1021/es203901u.
- Rodionov, A., Amelung, W., Peinemann, N., Haumaier, L., Zhang, X., Kleber, M., Glaser, B., Urusevskaya, I., Zech, W., 2010. Black carbon in grassland ecosystems of the world. Glob. Biogeochem. Cycles 24. https://doi.org/10.1029/2009gb003669.
- Romano, J.-C., Garabetian, F., 1996. Photographic records of sea-surface microlayers as a survey of pollution daily rhythm in coastal waters. Mar. Environ. Res. 41, 265–279. https://doi.org/10.1016/0141-1136(95)00019-4.
- Saiz, G., Wynn, J.G., Wurster, C.M., Goodrick, I., Nelson, P.N., Bird, M.I., 2015. Pyrogenic carbon from tropical savanna burning: production and stable isotope composition. Biogeosciences 12, 1849–1863. https://doi.org/10.5194/bg-12-1849-2015.
- Sánchez-García, L., Cato, I., Gustafsson, Ö., 2010. Evaluation of the influence of black carbon on the distribution of PAHs in sediments from along the entire Swedish continental shelf. Mar. Chem. 119, 44–51. https://doi.org/10.1016/j. marchem.2009.12.005.
- Santín, C., Doerr, S.H., Kane, E.S., Masiello, C.A., Ohlson, M., de la Rosa, J.M., Preston, C. M., Dittmar, T., 2016. Towards a global assessment of pyrogenic carbon from vegetation fires. Glob. Chang. Biol. 22, 76–91. https://doi.org/10.1111/gcb.12985.
- Schlitzer, R., 2023. Ocean Data View (Version 5.6.5). Available from. https://odv.awi.de.
 Schmitt-Kopplin, P., Liger-Belair, G., Koch, B.P., Flerus, R., Kattner, G., Harir, M.,
 Kanawati, B., Lucio, M., Tziotis, D., Hertkorn, N., Gebefügi, I., 2011. Dissolved organic matter in sea spray: a transfer study from marine surface water to aerosols.
- Biogeosci. Discuss. 8, 11767–11793. https://doi.org/10.5194/bgd-8-11767-2011. Seidel, M., Yager, P.L., Ward, N.D., Carpenter, E.J., Gomes, H.R., Krusche, A.V., Richey, J.E., Dittmar, T., Medeiros, P.M., 2015. Molecular-level changes of dissolved organic matter along the Amazon River-to-ocean continuum. Mar. Chem. 177, 218–231. https://doi.org/10.1016/j.marchem.2015.06.01.
- Schneider, E., Czech, H., Hansen, H.J., Jeong, S., Bendl, J., Saraji-Bozorgzad, M., Sklorz, M., Etzien, U., Buccholz, B., Streibel, T., Adam, T.W., Rüger, C.P., Zimmermann, R., 2023. Humic-like substances (HULIS) in ship engine emissions: molecular composition effected by fuel type, engine mode, and wet scrubber usage. Environ. Sci. Technol. 57 (37), 13948–13958. https://doi.org/10.1021/acs.est.3c04390.
- Seidel, M., Manecki, M., Herlemann, D.P.R., Deutsch, B., Schulz-Bull, D., Jürgens, K., Dittmar, T., 2017. Composition and transformation of dissolved organic matter in the Baltic Sea. Front. Earth Sci. China 5. https://doi.org/10.3389/feart.2017.00031.
- Serafim, T.S.G., Gomes de Almeida, M., Thouzeau, G., Michaud, E., Niggemann, J., Dittmar, T., Seidel, M., de Rezende, C.E., 2023. Land-use changes in Amazon and Atlantic rainforests modify organic matter and black carbon compositions transported from land to the coastal ocean. Sci. Total Environ. 878, 162917. https:// doi.org/10.1016/j.scitotenv.2023.162917.
- Shields, M.R., Bianchi, T.S., Osburn, C.L., Kinsey, J.D., Ziervogel, K., Schnetzer, A., Corradino, G., 2019. Linking chromophoric organic matter transformation with biomarker indices in a marine phytoplankton growth and degradation experiment. Mar. Chem. 214, 103665. https://doi.org/10.1016/j.marchem.2019.103665.
- Stubbins, A., Niggemann, J., Dittmar, T., 2012. Photo-lability of deep ocean dissolved black carbon. Biogeosciences 9, 1661–1670. https://doi.org/10.5194/bg-9-1661-2012
- Stubbins, A., Spencer, R.G.M., Mann, P.J., Holmes, R.M., McClelland, J.W., Niggemann, J., Dittmar, T., 2015. Utilizing colored dissolved organic matter to

- derive dissolved black carbon export by arctic rivers. Front. Earth Sci. 3. https://doi.org/10.3389/feart.2015.00063.
- Sun, H., Li, X., Zhu, C., Huo, Y., Zhu, Z., Wei, Y., Yao, L., Xiao, H., Chen, J., 2021. Molecular composition and optical property of humic-like substances (HULIS) in winter-time PM2.5 in the rural area of North China Plain. Atmos. Environ. 252, 118316. https://doi.org/10.1016/j.atmosenv.2021.118316.
- Tobiszewski, M., Namieśnik, J., 2012. PAH diagnostic ratios for the identification of pollution emission sources. Environ. Pollut. 162, 110–119. https://doi.org/10.1016/ j.envpol.2011.10.025.
- Vaezzadeh, V., Yi, X., Rais, F.R., Bong, C.W., Thomes, M.W., Lee, C.W., Zakaria, M.P., Wang, A.J., Zhong, G., Zhang, G., 2021. Distribution of black carbon and PAHs in sediments of Peninsular Malaysia. Mar. Pollut. Bull. 172, 112871. https://doi.org/10.1016/j.marpolbul.2021.112871.
- Vaezzadeh, V., Zhong, G., Gligorovski, S., Wang, Y., Zhang, G., 2023. Characteristics of dissolved black carbon in riverine surface microlayer. Mar. Pollut. Bull. 194, 115301. https://doi.org/10.1016/j.marpolbul.2023.115301.
- Venables, W.N., Ripley, B.D., 2002. Modern applied statistics with S. Stat. Comput. 4 (XII), 498. https://doi.org/10.1007/978-0-387-21706-2.
- Wagner, S., Riedel, T., Niggemann, J., Vähätalo, A.V., Dittmar, T., Jaffé, R., 2015. Linking the molecular signature of heteroatomic dissolved organic matter to watershed characteristics in world rivers. Environ. Sci. Technol. 49, 13798–13806. https://doi.org/10.1021/acs.est.5b00525.
- Wagner, S., Brandes, J., Spencer, R.G., Ma, K., Rosengard, S.Z., Moura, J.M.S., Stubbins, A., 2019. Isotopic composition of oceanic dissolved black carbon reveals non-riverine source. Nat. Commun. 10 (1), 5064. https://doi.org/10.1038/s41467-019-13111-7
- Wagner, S., Jaffé, R., Stubbins, A., 2018. Dissolved black carbon in aquatic ecosystems. Limnol. Oceanogr. Lett. 3, 168–185. https://doi.org/10.1002/lol2.10076.
- Wang, P., Mi, W., Xie, Z., Tang, J., Apel, C., Joerss, H., Ebinghaus, R., Zhang, Q., 2020. Overall comparison and source identification of PAHs in the sediments of European Baltic and North Seas, Chinese Bohai and Yellow Seas. Sci. Total Environ. 737, 139535. https://doi.org/10.1016/j.scitotenv.2020.139535.
- Wiedemeier, D.B., Brodowski, S., Wiesenberg, G.L.B., 2015. Pyrogenic molecular markers: linking PAH with BPCA analysis. Chemosphere 119, 432–437. https://doi. org/10.1016/j.chemosphere.2014.06.046.
- Wiriya, W., Prapamontol, T., Chantara, S., 2013. PM10-bound polycyclic aromatic hydrocarbons in Chiang Mai (Thailand): seasonal variations, source identification, health risk assessment and their relationship to air-mass movement. Atmos. Res. 124, 109–122. https://doi.org/10.1016/j.atmosres.2012.12.014.
- Witt, G., 2002. Occurrence and transport of polycyclic aromatic hydrocarbons in the water bodies of the Baltic Sea. Mar. Chem. 79, 49–66. https://doi.org/10.1016/ S0304-4203(02)00035-X.
- Witt, G., Matthäus, W., 2001. The impact of salt water inflows on the distribution of polycyclic aromatic hydrocarbons in the deep water of the Baltic Sea. Mar. Chem. 74, 279–301. https://doi.org/10.1016/s0304-4203(01)00020-2.
- Wolska, L., Zygmunt, B., Namieśnik, J., 2003. Organic pollutants in the Odra river ecosystem. Chemosphere 53, 561–569. https://doi.org/10.1016/S0045-6535(03) 00368-0
- Wu, Y.-L., Wang, X.-H., Li, Y.-Y., Hong, H.-S., 2011. Occurrence of polycyclic aromatic hydrocarbons (PAHs) in seawater from the Western Taiwan Strait, China. Mar. Pollut. Bull. 63, 459–463. https://doi.org/10.1016/j.marpolbul.2011.03.008.

- Wurl, O., Obbard, J.P., 2004. A review of pollutants in the sea-surface microlayer (SML): a unique habitat for marine organisms. Mar. Pollut. Bull. 48, 1016–1030. https://doi.org/10.1016/j.marpolbul.2004.03.016.
- Wurl, O., Miller, L., Vagle, S., 2011. Production and fate of transparent exopolymer particles in the ocean. J. Geophys. Res. Oceans 116 (C7). https://doi.org/10.1029/ 2011JC007342.
- Ya, M.-L., Wang, X.-H., Wu, Y.-L., Ye, C.-X., Li, Y.-Y., 2014. Enrichment and partitioning of polycyclic aromatic hydrocarbons in the sea surface microlayer and subsurface water along the coast of Xiamen Island, China. Mar. Pollut. Bull. 78, 110–117. https://doi.org/10.1016/j.marpolbul.2013.10.053.
- Yamashita, Y., Kojima, D., Yoshida, N., Shibata, H., 2021. Relationships between dissolved black carbon and dissolved organic matter in streams. Chemosphere 271, 129824. https://doi.org/10.1016/j.chemosphere.2021.129824.
- Yan, Z., Xin, Y., Zhong, X., Yi, Y., Li, P., Wang, Y., Zhou, Y., Zhou, Y., He, C., Shi, Q., He, D., 2023. Dissolved organic nitrogen cycling revealed at the molecular level in the Bohai and Yellow Sea. Water Res. 244, 120446. https://doi.org/10.1016/j. watres.2023.120446.
- Yan, Z., Xin, Y., Zhong, X., Yi, Y., Li, P., Wang, Y., Zhou, Y., He, Y., He, C., Shi, Q., Xu, W., He, D., 2024. Evolution of dissolved organic nitrogen chemistry during transportation to the marginal sea: insights from nitrogen isotope and molecular composition analyses. Water Res. 249, 120942. https://doi.org/10.1016/j. watres.2023.120942.
- Yang, J., Kang, S., Ji, Z., Chen, D., 2018. Modeling the origin of anthropogenic black carbon and its climatic effect over the Tibetan Plateau and surrounding regions. J. Geophys. Res. Atmos. 123 (2), 671–692. https://doi.org/10.1002/2017JD02728.
- Ytreberg, E., Hansson, K., Hermansson, A.L., Parsmo, R., Lagerström, M., Jalkanen, J.-P., Hassellöv, I.-M., 2022. Metal and PAH loads from ships and boats, relative other sources, in the Baltic Sea. Mar. Pollut. Bull. 182, 113904. https://doi.org/10.1016/j. marnolbul.2022.113904
- Yunker, M.B., Macdonald, R.W., Vingarzan, R., Mitchell, R.H., Goyette, D., Sylvestre, S., 2002. PAHs in the Fraser River basin: a critical appraisal of PAH ratios as indicators of PAH source and composition. Org. Geochem. 33, 489–515. https://doi.org/ 10.1016/s0146-6380(02)00002-5.
- Zhang, X., Wang, Y., Wang, Z., Zhao, M., Fang, Y., Ding, S., Xiao, W., Yu, C., Wang, X., Xu, Y., 2024. Heterogenous distribution and burial flux of black carbon in Chinese lakes and its global implication. Sci. Total Environ. 906, 167687. https://doi.org/10.1016/j.scitotenv.2023.167687.
- Zhang, Z., Cai, W., Liu, L., Chen, F., 2003. Direct determination of thickness of sea surface microlayer using a pH microelectrode at original location. Sci. China 46, 339. https://doi.org/10.1360/02yb0192.
- Zhao, M., Zhang, Y., Ma, W., Fu, Q., Yang, X., Li, C., Zhou, B., Yu, Q., Chen, L., 2013a. Characteristics and ship traffic source identification of air pollutants in China's largest port. Atmos. Environ. 64, 277–286. https://doi.org/10.1016/j. atmosenv.2012.10.007.
- Zhao, W., Bao, H., Huang, D., Niggemann, J., Dittmar, T., Kao, S.-J., 2023. Evidence from molecular marker and FT-ICR-MS analyses for the source and transport of dissolved black carbon under variable water discharge of a subtropical estuary. Biogeochemistry 162, 43–55. https://doi.org/10.1007/s10533-022-00987-9.
- Zhao, X.J., Zhao, P.S., Xu, J., Meng, W., Pu, W.W., Dong, F., He, D., Shi, Q.F., 2013b. Analysis of a winter regional haze event and its formation mechanism in the North China Plain. Atmos. Chem. Phys. Discuss. 13, 903–933. https://doi.org/10.5194/ acpd-13-903-2013.